Table I. Causative factors in 34 patients with Rasmussen syndrome.

	EPC type	Non-EPC type	Total
Age of onset	6.3 ± 5.6	8.7 ± 8.0	7.4 ± 6.7
Preceding infections	8 (40.0%)	5 (35.7%)	13 (38.2%)
Fever only	4	1	5
Upper respiratory infection	2	1	3
Influenza	1	2	3
Mycoplasma	0	1	1
Aseptic meningitis	1	0	1
Vaccination	1 (5.0%)	1 (7.1%)	2 (5.9%)
Head trauma	2 (10.0%)	1 (7.1%)	3 (8.8%)
None	9 (45.0%)	7(50.0%)	16(47.1%)
Total	20	14	34

Therefore, it remains unknown whether specific microbes are involved in the development of Rasmussen syndrome. The contribution of molecular mimicry between microbial and neuronal molecules and degeneracy of T cell receptor recognition to the development of Rasmussen syndrome (autoimmune-mediated epilepsies) will be discussed later.

We encountered two patients who developed Rasmussen syndrome after vaccination, although vaccination was not reported as a causative factor in the series of Montreal Neurological Institute. One patient had EPC type Rasmussen syndrome. This patient received Japanese encephalitis vaccination at the age of 15 years. Two months after vaccination, he had the initial epileptic seizure, and subsequently evolved to intractable and frequent complex partial seizures (CPSs) and EPC. MRI lesions in left frontal lobe and autoantibodies against GluRε2 were detected. Focal resection of the left frontal lobe failed to control epileptic seizures, psychiatric symptoms and deterioration. Another patient had non-EPC type Rasmussen syndrome. This patient received measles–mumps–rubella triple vaccine at the age of 1 year. Three weeks later, he was affected by aseptic meningitis caused by the vaccination. He had intractable epileptic seizures from the age of two, and psychiatric symptoms (including anxiety) evolved subsequently. At the age of 14 years, right frontal lobectomy was conducted and successfully controlled the seizures.

Head trauma also was not reported as a causative factor in the patients of Montreal Neurological Institute, but we identified three patients with Rasmussen syndrome possibly related to preceding head trauma. As we sometimes experience patients with aseptic meningitis after head trauma, head trauma may facilitate the invasion of inflammatory T cells into the CNS. In patients with post-concussion syndrome after mild head injury, focal cortical dysfunction may occur in conjunction with the disruption of the blood brain barrier (Korn et al. 2005).

In the following sections, infection as a causative factor in Rasmussen syndrome will be illustrated using a specific case in which Rasmussen syndrome developed after influenza infection, especially focusing on the roles of molecular mimicry and HLA class I.

A case of Rasmussen syndrome after influenza A infection, and cross-reaction of lymphocytes

This patient, a boy, was 8 year-old at the time of this report (Case 1). His family history was unremarkable, with ovarian cyst in his mother and parkinsonism in his maternal grandfather. At the age of 3 years and 11 months, he had febrile generalized convulsion following an episode of influenza A infection that was confirmed by antigen detection from a nasal sample. Before the influenza infection, he had no neurological symptoms and no other preceding conditions that might precipitate the convulsions. Soon after the initial convulsion, at age 4, he had febrile convulsive status of left extremities associated with repeated influenza A infection. CSF was normal, and CT revealed no abnormalities. At the age of 4 years and 1 month, afebrile convulsive status appeared and phenobarbital (50 mg) was prescribed. Thereafter, his seizures became progressively intractable, in spite of a combination of several antiepileptic drugs (carbamazepine, zonisamide, valproic acid and phenytoin). At the age of 5 years and 4 months, EPC appeared after phenytoin was stopped abruptly and clobazam was added. He was referred to our epilepsy center for the treatment of Rasmussen syndrome at the age of 5 years and 5 months. He had hemiparesis of left extremities, EPC of left lower extremity, and several partial seizures in a day (Figure 4). After functional hemispherectomy, seizures were controlled completely. At age eight, he walked to school and attended a normal elementary school.

At presentation, IgG-autoantibodies against GluRε2 were detected in serum and CSF samples (Takahashi et al. 2003), but IgM-autoantibody was negative. The stimulation index obtained in the lymphocyte stimulation test (LST) stimulated with homogenates containing GluRε2 (^{3}H-thymidine

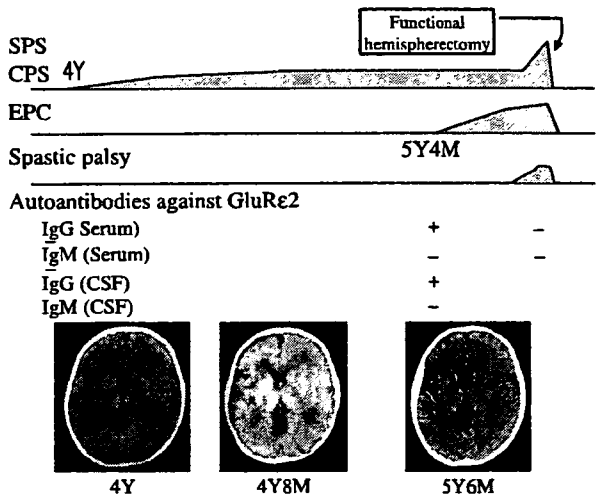

Figure 4. Clinical course of Case 1. Epilepsy occurred at the age of four, and progressive atrophy of right hemisphere started at the age of 5 year and 6 months. IgG-autoantibodies against GluRε2 were positive on admission, but became negative after functional hemispherectomy that successfully controlled seizures. SPS, simple partial seizure; CPS, complex partial seizure; EPC, epilepsia partialis continua.

uptake with stimulation/control ^{3}H-thymidine uptake) was 2.78 (Takahashi et al. 2005), and was higher than normal controls (0.63, 1.67) tested simultaneously (Figure 5). When LST was conducted by co-stimulation with homogenates containing GluRε2 and influenza vaccine, the stimulation index was 9.19 in this patient (Case 1 in Figure 5), and was

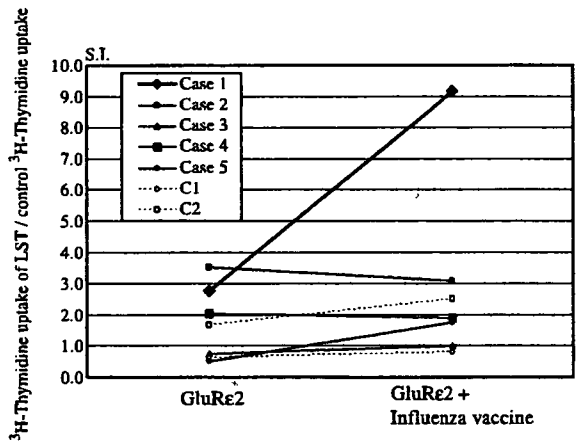

Figure 5. Stimulation index in lymphocyte stimulation test. Data on the left show stimulation indices (SI) (^{3}H-thymidine uptake with stimulation/control ^{3}H-thymidine uptake) obtained in lymphocyte stimulation test (LST) stimulated with homogenate containing GluRε2 (Takahashi et al. 2005). Data on the right show SI when LST was conducted by co-stimulation with homogenates containing GluRε2 and influenza vaccine. Case 1 is the case presented in the text, with influenza A infection as a causative factor. Case 2 is Rasmussen syndrome with no causal relationship with influenza. Cases 3–5 are epileptic cases (no Rasmussen syndrome) with autoantibodies against GluRε2. C1 and C2 are normal controls.

higher compared with other patients with Rasmussen syndrome or other epilepsies not related to preceding influenza infection (Cases 2–5). A synergistic increase in stimulation index with co-stimulation (GluRε2 + influenza vaccine) compared to GluRε2 stimulation alone was observed only in the present case. These data suggest that the lymphocytes of this patient are sensitized not only by influenza antigen but also by GluRε2, and that the T cell receptors of this patient can cross-react with peptides from influenza and GluRε2.

After the T cell receptors on CTLs recognize both the HLA class I molecule and its binding peptide expressed on antigen presenting cells (APCs), these CTLs are activated into cytotoxic effector cells that are capable of invading the CNS. If through molecular mimicry and T cell receptor redundancy, the CTLs activated by microbial peptides are able to recognize the HLA class I and binding peptide expressed on neurons, then the infection-activated CTLs may induce apoptosis of neurons. Therefore, HLA class I is one of the key molecules that determines autoimmune mechanisms underlying the process leading from infection or vaccination to Rasmussen syndrome.

HLA class I and theoretical cross-reaction of CTLs in Case 1

In the case presented above (Case 1), HLA genotyping identified HLA – A*0201, A*2402, and B*3501 (homo). HLA – A*0201 binds peptides with the following motif: [LM] – x(3) – V – x(2) – [VL] (x, free amino acid; L, leucine; M, methionine; V, valine). Database analyses (Genome Net: http://www.genome.jp/) revealed this motif in various viral molecules and neural molecules (Figure 6). If patients with HLA – A*0201 are infected by influenza A virus, the peptide *LAIMVAGL* from the hemagglutinin of influenza A is able to bind with A*0201 expressed on APCs. CTLs with T cell receptors that recognize A*0201 and the hemagglutinin peptide (influenza A) on APCs become activated and become effector CTLs. Theoretically, these effector CTLs can invade the CNS, and react with neurons expressing HLA – A*0201 and peptides containing the [LM] – x(3) – V – x(2) – [VL] motif, due to molecular mimicry and degeneracy of T cell receptor recognition (Uemura et al. 2003). Peptides having the HLA – A*0202 binding motif are found in various neuronal molecules, such as GluRε2 (*LVLAVLAV*, *MLLIVSAV*) and GluRε1 (*L*PLD*V*NV*V*). Therefore, we hypothesize that CTLs activated by influenza may cross-react with neurons that express GluRε2 under specific conditions such as the presence of costimulators. This hypothetic cross-reaction based on molecular mimicry of HLA-binding motif is compatible with our data of

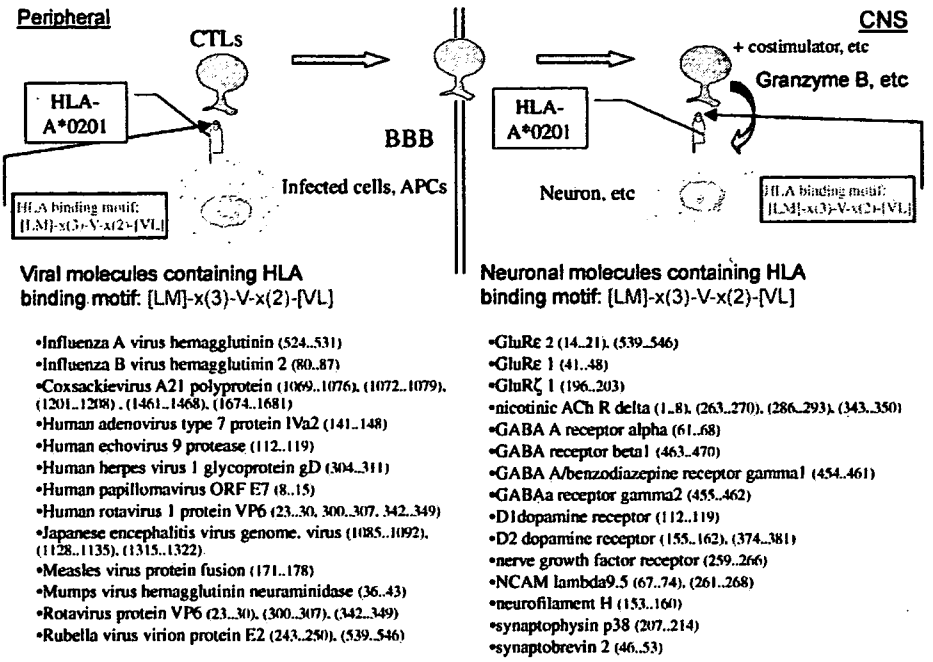

Figure 6. Viral and neural molecules containing specific binding motif for HLA − A*0201. Viral infection of host cells leads to expression of some parts of the viral peptides by binding with HLA class I molecule on the infected cells. CTLs expressing T cell receptors that recognize the peptide and HLA class I are activated, resulting in generation of effecter T cells. In individuals with HLA − A*0201, the binding motif is [LM] − *x*(3) − V − *x*(2) − [VL] (*x*, free amino acid; L, leucine; M, methionine; V, valine). Database analyses (Genome Net, http://www.genome.jp/) revealed many viral molecules containing this motif, as shown in the left column. The numbers in parentheses are sequence numbers indicating the sites of the motif. Effecter T cells are able to cross the blood brain barrier to reach the CNS, and theoretically can cross-react with neurons expressing the same motif on HLA class I, under specific conditions such as the presence of costimulator. Database analyses revealed many neural molecules including NMDA-GluRs, which contain the motif, as shown in the right column.

lymphocyte cross-reactivity between GluRε2 and influenza vaccine observed in Case 1 (Figure 5). Since CTLs activated by influenza can react with a broad spectrum of neuronal molecules, theoretically, apoptotic lesions caused by CTLs may distribute widely in the brain. On the other hand, possible interactions of the activated CTLs of Case 1 with a variety of microbial molecules (Figure 6) may explain the symptomatic aggravation triggered by infections other than influenza after the onset of Rasmussen syndrome. T cell clones from type 1 diabetes patients have been shown to react with several kinds of microbial mimicry peptides (Uemura et al. 2003). Similar molecular mimicry may also exists for HLA − A*2402 and B*3501. These molecules also have specific binding motifs. Database search identified diverse peptides containing these specific motifs in both microbial and neural molecules.

HLA class I in patients with Rasmussen syndrome

We studied the genotypes of HLA class I in 16 Japanese patients with Rasmussen syndrome (EPC type, 9; non-EPC type, 7) by PCR amplifications. The data were analyzed statistically using Chi-square for independence test. HLA − A*2402 is a popular genotype (36.5% of Japanese population) and was found in 77.8% of EPC type patients ($p = 0.016$). The frequencies of HLA − A*0201 and HLA − A*2601 were higher in non-EPC type patients (both 42.9%) than in Japanese population (10.7 and 11.3%, respectively) ($p = 0.033$ and 0.038, respectively). HLA − B*5201was found more frequently in EPC type patients (33.3%) than in Japanese population (10.9%) ($p = 0.070$), while HLA − B*4601 was more frequent in non-EPC type patients (28.6%) than in Japanese population (3.4%) ($p = 0.025$). The relative risks of various HLA class I genotypes for Rasmussen syndrome range from 6 to 11 (Table II), which are at the same levels as systemic lupus erythematosus (DR2) and acute anterior uveitis (B27) (Marsh et al. 2000). The relative risks of HLA class I-A and B haplotypes range from 5 to ∞. Since the haplotype of A*2601 + B*5401 was not observed in 561 Japanese subjects, the risk is infinity.

The HLA class I types that have higher relative risks may have a greater potential to induce cross-reactions of CTLs between microbes and neurons, and consequently may be found at higher frequencies in patients with Rasmussen syndrome. The binding motifs of these HLA class I types probably exist frequently in molecules from microbes commonly found in Japan and in molecules derived from neurons.

Table II. HLA class I genotypes and relative risks in patients with Rasmussen syndrome.

HLA genotypes	Clinical phenotype	Relative risk
HLA class I-A		
A*2402	EPC type	6.1
A*0201	Non-EPC type	6.4
A*2601	Non-EPC type	6.3
HLA class I-B		
B*4601	Non-EPC type	11.4
HLA − A + B haplotypes		
A*2402 + B*4801	EPC type	13.3
A*2402 + B*1501	EPC type	21.1
A*2402 + B*5201	EPC type	5.1
A*2601 + B*5401	Non-EPC type	∞

∞, infinity.

Acknowledgements

The author thanks Masayoshi Mishina and Hisashi Mori for their helpful comments, and Shigeko Nishimura and Hisano Tsunogae for their skillful assistance. This study was funded in part by Research Grants (16A-3) for Nervous and Mental Disorders from the Ministry of Health, Labor and Welfare, grants-in-aid for Scientific Research I No. 15591151, 16590859, and 17591133, Health and Labour Sciences Research Grants for Research on Psychiatry and Neurological Diseases and Mental Health (H17-017) and Research on Children and Families (H16-016), and grants from The Japan Epilepsy Research Foundation.

References

Aguilar MJ, Rasmussen T. 1960. Role of encephalitis in pathogenesis of epilepsy. AMA Arch Neurol 2:663–676.

Andermann F, editor. 1991. Chronic encephalitis and epilepsy: Rasmussen's syndrome. Boston: Butterworth-Heinemann.

Bien CG, Bauer J, Deckwerth TL, et al. 2002a. Destruction of neurons by cytotoxic T cells: A new pathogenic mechanism in Rasmussen's encephalitis. Ann Neurol 51:311–318.

Bien CG, Widman G, Urbach H, et al. 2002b. The natural history of Rasmussen's encephalitis. Brain 125:1751–1759.

Farrell MA, Droogan O, Secor DL, Poukens V, Quinn B, Vinters HV. 1995. Chronic encephalitis associated with epilepsy: Immunohistochemical and ultrastructural studies. Acta Neuropathol 89:313–321.

He XP, Patel M, Whitney KD, Janumpalli S, Tenner A, McNamara JO. 1998. Glutamate receptor GluR3 antibodies and death of cortical cells. Neuron 20:153–163.

Korn A, Golan H, Melamed I, Pascual-Marqui R, Friedman AJ. 2005. Focal cortical dysfunction and blood–brain barrier disruption in patients with Postconcussion syndrome. Clin Neurophysiol 22:1–9.

Levite M, Hermelin A. 1999. Autoimmunity to the glutamate receptor in mice—a model for Rasmussen's encephalitis? J Autoimmun 13:73–82.

Li Y, Uccelli A, Laxer KD, et al. 1997. Local-clonal expansion of infiltrating T lymphocytes in chronic encephalitis of Rasmussen. J Immunol 158:1428–1437.

Marsh SGE, Parham P, Barber LD. 2000. The HLA factsBook. London: Academic Press. p 79–83.

Rogers SW, Andrews PI, Gahring LC, et al. 1994. Autoantibodies to glutamate receptor GluR3 in Rasmussen's encephalitis. Science 265:648–651.

Roubertie A, Boukhaddaoui H, Sieso V, et al. 2005. Antiglial cell autoantibodies and childhood epilepsy: A case report. Epilepsia 46:1308–1312.

Takahashi Y. 2006. Vaccination and infection as causative factors of epilepsy. Future Neurol (in press).

Takahashi Y, Mori H, Mishina M, et al. 2003. Autoantibodies to NMDA receptor in patients with chronic forms of epilepsia partialis continua. Neurology 61:891–896.

Takahashi Y, Mori H, Mishina M, et al. 2005. Autoantibodies and cell-mediated autoimmunity to NMDA-type GluRε2 in patients with Rasmussen's encephalitis and chronic progressive epilepsia partialis continua. Epilepsia 46(Suppl 5):152–158.

Twyman RE, Gahring LC, Spiess J, Rogers SW. 1995. Glutamate receptor antibodies activate a subset of receptors and reveal an agonist binding site. Neuron 14:755–762.

Uemura Y, Senju S, Maenaka K, et al. 2003. Systematic analysis of the combinatorial nature of epitopes recognized by TCR leads to identification of mimicry epitopes for glutamic acid decarboxylase 65-specific TCRs. J Immunol 170:947–960.

Watson R, Jiang Y, Bermudez I, et al. 2004. Absence of antibodies to glutamate receptor type 3 (GluR3) in Rasmussen encephalitis. Neurology 63:43–50.

Watson R, Lang B, Bermudez I, et al. 2001. Autoantibodies in Rasmussen's encephalitis. J Neuroimmunol 118:148.

Xiong ZO, McNamara JO. 2002. Fleeting activation of ionotropic glutamate receptors sensitizes cortical neurons to complement attack. Neuron 36:363–374.

Xiong ZO, Qian W, Suzuki K, McNamara JO. 2003. Formation of complement membrane attack complex in mammalian cerebral cortex evokes seizures and neurodegeneration. J Neurosci 23: 955–960.

Yang R, Puranam RS, Butler LS, et al. 2000. Autoimmunity to munc-18 in Rasmussen's encephalitis. Neuron 28:375–383.

SHORT REPORT

Anti-Ma2 associated paraneoplastic neurological syndrome presenting as encephalitis and progressive muscular atrophy

M Waragai, A Chiba, A Uchibori, T Fukushima, M Anno, K Tanaka

J Neurol Neurosurg Psychiatry 2006;**77**:111–113. doi: 10.1136/jnnp.2005.068775

A 36 year old man with a history of testicular germ cell tumour presented six months after bilateral orchidectomy with progressive amnesia, irritability, vertical gaze palsy, and generalised seizures. Eight months after initial onset of symptoms, he demonstrated a head drop with muscular atrophy of the upper limbs, shoulder girdle, and posterior neck. He reported no sensory disturbances and his sensory examination was normal. The overall clinical presentation was consistent with motor neurone disease. Cerebrospinal fluid analysis revealed mild pleocytosis and increased protein concentration. Serum and cerebrospinal fluid were positive for the anti-Ma2 antibody by western blot analysis and immunostaining. Abnormal high signal in the grey matter was noted in the cervical spinal cord and brain by T2 weighted magnetic resonance imaging (MRI). The patient was treated with corticosteroids, intravenous immunoglobulin, and antiepileptic medication. The patient improved clinically and symptom progression ceased after initiation of treatment. There was complete resolution of the abnormal brain MRI lesions; however, the cervical spinal cord MRI lesion and muscular atrophy remained unchanged. It is suggested that the anti-Ma2 antibody is involved not only in encephalitis, but may also play a role in the cervical spinal cord lesions resulting in a motor neurone disease-like presentation.

Paraneoplastic neurological syndromes including paraneoplastic limbic encephalitis are neurological disorders that occur in patients with cancer.[1–3] Paraneoplastic limbic encephalitis is often associated with small cell lung carcinoma and testicular germ cell tumours.[1–3]

Recently, it was suggested that anti-Ma2 associated encephalitis differs from classic paraneoplastic limbic encephalitis because of its variable clinical features.[4]

Here, we report the clinical and neuroradiological findings in a patient with an anti-Ma2 associated paraneoplastic neurological syndrome who presented with encephalitis and progressive muscular atrophy.

To our knowledge, this is the first report describing the unique clinical features of a cervical spinal cord lesion confirmed by magnetic resonance imaging (MRI) in a patient with anti-Ma2 associated paraneoplastic neurological syndrome.

CASE REPORT

A 36 year old man was admitted to our hospital for progressive amnesia, hypersomnia, diplopia, and generalised convulsions in September 2003.

He had undergone a bilateral orchidectomy for testicular germ cell tumour six months before presentation. There was no recurrence of the tumour noted at the time of presentation.

On admission, the patient presented with confusion and seizures. There was no cerebellar ataxia or sensory disturbance noted on examination. Progressive muscular atrophy, weakness, and fasciculations of the upper extremities, shoulder girdle, and neck began eight months after initial presentation. Thereafter, he developed flaccid paralysis of the upper extremities and a head drop. A Babinski's sign was present bilaterally.

Cerebrospinal fluid (CSF) contained 5×10^3 lymphocytes/litre and 830 mg protein/litre. There were no atypical lymphocytes or tumour-like cells noted in the CSF. IgM titres for herpes simplex were negative. Muscle computed tomography at the level of C5 demonstrated severe muscular atrophy of the limb, shoulder girdle, paraspinal, and thoracic muscles. Electromyogram studies showed neurogenic changes in the muscles of the upper extremities and shoulder girdle, including the deltoid, biceps, triceps, scapular, and upper paraspinal muscles, and no changes to the muscles of the lower extremities and pelvic girdle. The results of a nerve conduction study, including sensory and motor evoked potentials, were within the normal ranges for all extremities.

Brain MRI revealed high signal intensity in the grey matter of the right frontal and bilateral mesial temporal lobes (fig 1A, B). T2 weighted MRI revealed high signal intensity in the grey matter of the cervical spinal cord (fig 1C, D). Serum and CSF were positive for the anti-Ma2 antibody confirmed by the binding to the recombinant Ma-2 protein, but were negative for anti-Ma1, anti-Hu, and anti-Yo antibodies (fig 2A, B). Thus, the patient was diagnosed as having an anti-Ma2-associated paraneoplastic neurological syndrome. The patient was treated with two courses of intravenous immunoglobulin (2.5 g/day for five days), followed by intravenous methylprednisolone (1 g/day for three days) during which the patient showed clinical improvement. The patient stabilised and progression of the muscular atrophy ceased, although he continued to have severe flaccid paralysis of the upper extremities and a head drop. The symptoms of amnesia, irritability, overall cognitive decline, hypersomnia, and vertical gaze palsy also remained unchanged. The patient was subsequently treated with antiepileptic medication to prevent further seizure activity. Brain MRI abnormalities resolved after the course of treatment, but the MRI cervical cord lesion remained.

Abbreviations: CSF, cerebrospinal fluid; MRI, magnetic resonance imaging

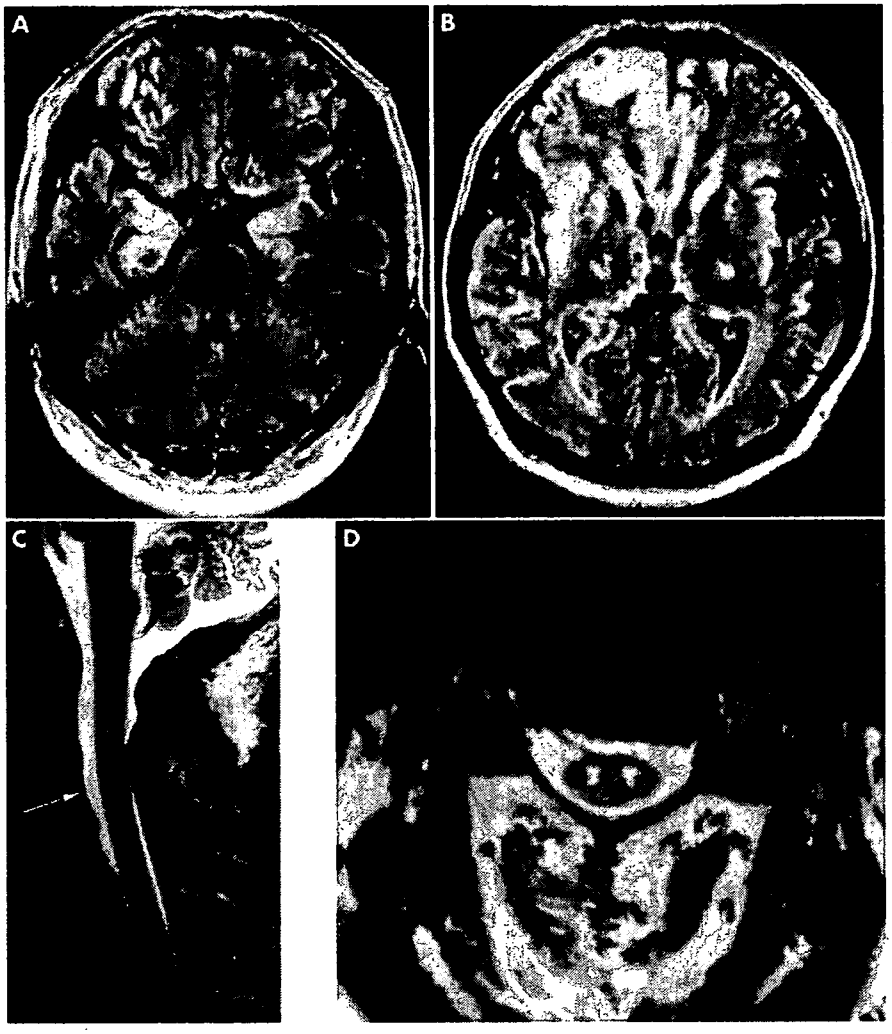

Figure1 (A, B) The magnetic resonance imaging (MRI) fluid attenuated inversion recovery image on admission demonstrated a high signal intensity in the bilateral mesial temporal lobe, right frontal cortex, and right insula. There was no enhancement by gadolinium-DTPA (diethylene triamine pentaacetic acid). These abnormal signal lesions disappeared following treatment with intravenous immunoglobulin and steroids. (C, D) T2 weighted MRI demonstrated a symmetrical high signal lesion (arrow), which was relatively confined to the grey matter of the cervical spinal cord. The lesion was not enhanced by gadolinium-DTPA.

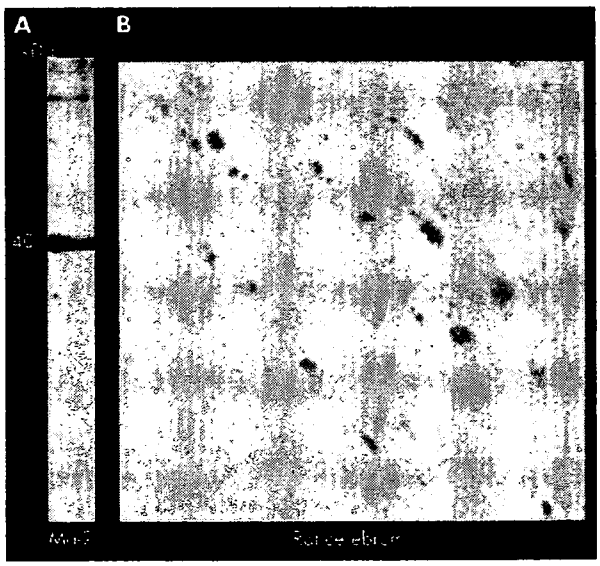

Figure 2 (A) Western blotting analysis showed that the patient's serum reacts with the 40 kDa protein band representing recombinant Ma-2 protein. (B) Immunostaining using the patient's serum and rat cerebrum shows nucleolar rather than nuclear staining.

DISCUSSION

We report the case of an anti-Ma2 associated paraneoplastic neurological syndrome in a patient with a history of testicular germ cell tumour who presented with encephalitis and motor neurone disease-like features. T2 weighted MRI of the cervical spinal cord showed a well confined high signal intensity lesion, which correlated with the extensive muscular atrophy and weakness.

Dalmau *et al* studied the clinical findings of 38 patients with anti-Ma2-associated encephalitis.[6] They reported that eye movement abnormalities were prominent in 92% of the patients with brainstem dysfunction, and 60% of these patients had vertical gaze paresis. Among 34 patients with cancer, 18 had testicular germ cell tumours. They concluded that anti-Ma2 encephalitis should be suspected in patients with limbic, diencephalic, or brainstem dysfunction who have MRI abnormalities in these regions and CSF inflammatory changes. In young male patients who present with paraneoplastic neurological syndromes, the primary tumour is usually located in the testis.[6] Dalmau *et al* also described a 58 year old man with adenocarcinoma of the lung, who developed proximal weakness, muscular atrophy, and fasciculations of the upper extremities without evidence of MRI abnormalities in the brain or spinal cord.[6] Our patient's presentation was characterised not only by encephalitis, but

also by motor neurone disease-like clinical features, which are probably attributable to the cervical spinal cord lesion.

Although it remains unclear whether the anti-Ma2 antibody associated with testicular germ cell tumours is directly involved in the pathogenesis of encephalitis and cervical spinal cord lesions, the response to immunomodulatory treatments such as intravenous immunoglobulin and steroids supports the idea that anti-Ma2 has anti-tumour immune activity.

Our case supports the unique clinical diversity of the anti-Ma2-associated paraneoplastic neurological disorder.

Authors' affiliations
M Waragai, T Fukushima, Division of Neurology, JR Tokyo General Hospital, 2-1-3, Yoyogi, Shibuya-ku, Tokyo 151-8528, Japan
A Chiba, A Uchibori, Department of Neurology, Kyorin University School of Medicine, Mitaka-shi, Tokyo 181-8611, Japan
M Anno, Department of Neurology, Tokyo Metropolitan Matsuzawa Hospital, Tokyo 156-0057, Japan
K Tanaka, Department of Neurology, Brain Research Institute, Niigata University, Niigata 951-8585, Japan

Competing interests: none declared

The patient gave full consent for this report to be published

Correspondence to: Dr M Waragai, Division of Neurology, JR Tokyo General Hospital, 2-1-3, Yoyogi, Shibuya-ku, Tokyo 151-8528, Japan; waragaram2002@aol.com

Received 29 March 2005
Revised form received 25 April 2005
Accepted 3 May 2005

REFERENCES

1 **Voltz R,** Gultekin SH, Rosenfeld MR, *et al.* A serologic marker of paraneoplastic limbic and brain-stem encephalitis in patients with testicular cancer. *N Engl J Med* 1999;340:1788–95.
2 **Barnett M,** Prosser J, Sutton I, *et al.* Paraneoplastic brain stem encephalitis in a woman with anti-Ma2 antibody. *J Neurol Neurosurg Psychiatry* 2001;70:222–5.
3 **Rosenfeld MR,** Eichen JG, Wade DF, *et al.* Molecular and clinical diversity in paraneoplastic immunity to Ma proteins. *Ann Neurol* 2001;50:339–48.
4 **Sahashi K,** Sakai K, Mano K, *et al.* Anti-Ma2 antibody related paraneoplastic limbic/brain stem encephalitis associated with breast cancer expressing Ma1, Ma2, and Ma3 mRNAs. *J Neurol Neurosurg Psychiatry* 2003;74:1332–5.
5 **Scheid R,** Lincke T, Voltz R, *et al.* Serial 18F-fluoro-2-deoxy-D-glucose positron emission tomography and magnetic resonance imaging of paraneoplastic limbic encephalitis. *Arch Neurol* 2004;61:1785–9.
6 **Dalmau J,** Graus F, Villarejo A, *et al.* Clinical analysis of anti-Ma2-associated encephalitis. *Brain* 2004;127:1831–44.

JOURNAL OF CLINICAL MICROBIOLOGY, Feb. 2005, p. 951–955 Vol. 43, No. 2
0095-1137/05/$08.00+0 doi:10.1128/JCM.43.2.951–955.2005

Rapid Diagnosis of Herpes Simplex Virus Infection by a Loop-Mediated Isothermal Amplification Method

Yoshihiko Enomoto,[1] Tetsushi Yoshikawa,[1]* Masaru Ihira,[2] Shiho Akimoto,[1] Fumi Miyake,[1] Chie Usui,[1] Sadao Suga,[1] Kayoko Suzuki,[3] Takashi Kawana,[4] Yukihiro Nishiyama,[5] and Yoshizo Asano[1]

Department of Pediatrics, Fujita Health University School of Medicine,[1] and Department of Medical Information Technology, Fujita Health University College,[2] Toyoake, and Department of Dermatology, Central Hospital of Tokai Medical Institute, Tokai,[3] and Department of Virology, Nagoya University Graduate School of Medicine, Nagoya,[5] Aichi, and Department of Obstetrics and Gynecology, University Hospital, Mizonokuchi, Teikyo University School of Medicine, Kawasaki, Kanagawa,[4] Japan

Received 1 March 2004/Returned for modification 3 May 2004/Accepted 12 October 2004

Primers for herpes simplex virus type 1 (HSV 1)-specific loop-mediated isothermal amplification (LAMP) method amplified HSV-1 DNA, while HSV-2-specific primers amplified only HSV-2 DNA; no LAMP products were produced by reactions performed with other viral DNAs. The sensitivities of the HSV-1- and HSV-2-specific LAMP methods, determined by agarose gel electrophoresis, reached 500 and 1,000 copies/tube, respectively. The turbidity assay, however, determined the sensitivity of the HSV-1- and HSV-2-specific LAMP methods to be 1,000 and 10,000 copies/tube, respectively. After initial validation studies, 18 swab samples (in sterilized water) collected from patients with either gingivostomatitis or vesicular skin eruptions were examined. HSV-1 LAMP products were detected by agarose gel electrophoresis in the 10 samples that also demonstrated viral DNA detection by real-time PCR. Nine of these 10 samples exhibited HSV-1 LAMP products by turbidity assay. Furthermore, both the agarose gel electrophoresis and the turbidity assay directly detected HSV-1 LAMP products in 9 of the 10 swab samples collected in sterilized water. Next, we examined the reliability of HSV type-specific LAMP for the detection of viral DNA in clinical specimens (culture medium) collected from genital lesions. HSV-2 was isolated from all of the samples and visualized by either agarose gel electrophoresis or turbidity assay.

Viral isolation and serological assays are standard methods of herpes simplex virus (HSV) diagnosis. Both viral isolation and serological testing, however, require substantial time to obtain accurate final results. More rapid detection has been achieved by modification of cell culture techniques by centrifugation of inocula on cell monolayers and the use of immunofluorescence techniques (6). Recent studies have suggested that detection of HSV DNA by PCR increases the sensitivity of viral infection detection compared to antigenic detection or cell culture methods (3, 4, 11, 13, 14). While quantitative analysis of viral DNA by real-time PCR may become a valuable tool for bedside monitoring of HSV infection and progression (1, 2, 7, 10, 17, 21, 22), it has not yet become a common procedure in hospital laboratories due to the requirement of specific expensive equipment (a thermal cycler).

Recently, Notomi et al. (18) reported a novel nucleic acid amplification method, termed loop-mediated isothermal amplification (LAMP), which is used to amplify DNA under isothermal conditions with high specificity, efficiency, and speed. The most significant advantage of LAMP is the ability to amplify specific sequences of DNA between 63 and 65°C without thermocycling. Thus, the technique requires only simple and cost-effective equipment amenable to use in hospital laboratories. The LAMP method also exhibits both high specificity and high amplification efficiency. As the LAMP method uses four primers which recognize six distinct target DNA sequences, the specificity is extremely high. This method also exhibits extremely high amplification efficiency, due in part to its isothermal nature; as there is no time lost due to changes in temperature and the reaction can be conducted at the optimal temperature for enzyme function, the inhibition reactions that often occur at later stages of typical PCR amplifications are less likely to occur. Thus, this method could potentially be a valuable tool for the rapid diagnosis of infectious diseases (5, 8, 9, 12, 19, 23) in both commercial and hospital laboratories. In this study, we sought to establish a LAMP-based HSV type-specific DNA amplification method and examine its reliability for the detection of HSV DNA from clinical specimens.

HSV-1 (KOS) DNA and HSV-2 (186) DNA were used as positive controls to determine the appropriate conditions for HSV type-specific LAMP and to establish the baseline sensitivity and specificity levels. HSV-1 (KOS), HSV-2 (186), varicella-zoster virus (VZV) (Oka), human cytomegalovirus (HCMV) (AD-169), human herpesvirus type 6B (HHV-6B) (Z29), and HHV-7 (RK) DNA were used to determine the specificity of HSV type-specific LAMP. Plasmids containing

* Corresponding author. Mailing address: Department of Pediatrics, Fujita Health University School of Medicine, Toyoake, Japan 4701192. Phone: 8 1-562-939251. Fax: 8 1-562-95-2216. E-mail: tetsushi@fujita-hu.ac.jp.

TABLE 1. Primers targeting the HSV-1 and HSV-2 gG genes[a]

Virus	Locations of target sequences[b]	Name of primer	Sequence of primer[c]
HSV-1			
	136741 ATCATGTCGCAGGGCGCCATGCGTGGCGTTGTTCCCATTATCCCATTCCTTTGGTTCTT	HS1F3	5′-GCCGTTGTTCCCATTATCCC-3 (F3)
	136801 GTCGGT GTATCGGGGGTTCCCACCAA CGTCTCCTCCACCACCCAAGCCCAACTCCAGACC	HS1B3	5′-TACTTGGCATGGGGGGTG-3′ (B3c)
	136861 ACCGGTCGTCCCTCGCATGAAGGCCCCAAGATGACCAGAGCCGGCACCACCGAACTCTCCC	HS1F1P	5′-GTTGGGTGGTGGAGGAGACGTCCTTTTGGTTCTTGTCGGT-3′ (F1c-F2)
	136921 ACCGCCATCAGCCTTACCAGCGCCGACCACACACCCCCCATGCCAAGTATTGGACTGGAG	HS1B1P	5′-GGTCGTCCCTCGCATGAAGCGGCGTGGTAAGGCTGATG-3′ (B1-B2c)
		HS1LPF	5′-TTGGTGGGAACCCCCGATAC-3′ (LPFc)
		HS1LPB	5′-AACATGACCCAGACCGGCAC-3′ (LPB)
HSV-2			
	138901 CGCCTCATGGCCTTGACCGAGGACAC GTCCTCGATTCGCCTACGTCCCGCTCCGGAGAAG	HS2F3	5′-GGCCTTGACCGAGGACAC-3′ (F3)
	138961 ACGCCCCTCCCCTGTGTCGCCACCGCCATGGCACCCTCAGTCGACCCAAGCGCGGAACCG	HS2B3	5′-CGACTCCACGGATGCAGT-3′ (B3c)
	139021 ACCGCCCCCCGCAACCACTACTCCCCCCGACGAGATGGCCACACAAGCCGCAACGGTCGCC	HS2F1P	5′-TCGACTGAGGGTGCCATGGCGTCCTCCGATTCGCCTACG-3′ (F1c-F2)
	139081 GTTACGCCGGAGGAAACGGCAGTCGCCTCCCCCCGCCGCGACTGCATCCGTGGAGTCGTCG	HS2B1P	5′-GCAACCACTACTCCCCCCGACCGTTTCCTCCGGCGTAA-3′ (B1-B2c)
		HS2LPF	5′-GCCGACACACAGGGAGGGGCGT-3′ (LPFc)
		HS2LPB	5′-GATGGCCACACAAGCCGCAA-3′ (LPB)

[a] Names and sequences of each primer used for HSV type-specific LAMP are shown, as are locations of target sequences within the gG genes of HSV-1 and HSV-2. B2c, sequence complementary to B2; F1c, sequence complementary to F1; LPFc, sequence complementary to LPF; B3c, sequence complementary to B3.
[b] Numbers at left of sequences are nucleotide positions. GenBank accession numbers are as follows: NC001806 (HSV-1 complete genome) and NC001798 (HSV-2 complete genome).
[c] Designations in parentheses correspond to definitions and sequences described in footnote *a*.

the HSV-1 and HSV-2 target sequences were used to determine the assay sensitivity.

To determine the reliability of HSV type-specific LAMP for detection of viral DNA from clinical samples, 18 swab samples (sample numbers 1 to 18) were collected from patients with either gingivostomatitis or vesicular skin eruptions. Swabs were collected from patients at the outpatient clinic of the Fujita Health University hospital and the Central Hospital of the Tokai Medical Institute and placed into 1 ml of sterilized water. Five swab samples (sample numbers 19 to 23) were also collected from patients with genital herpes at Teikyo University Mizonokuchi Hospital outpatient clinic. Swabs were collected from the lesions and placed into culture medium. HSV-2 was isolated from all of these samples. We attempted detection of HSV-1 and HSV-2 DNA from either post-DNA extraction or without DNA extraction by using HSV-1-specific and HSV-2-specific LAMP. The results of HSV type-specific LAMP were compared with results obtained by the previously established technique of HSV type-specific real-time PCR to assess the reliability of the methods for the rapid diagnosis of HSV infection.

LAMP reactions were conducted as described previously by Notomi et al. (18) and Nagamine et al. (16). The LAMP method requires a set of four primers (B3, F3, BIP, and FIP) that recognize a total of six distinct sequences (B1 to B3 and F1 to F3) within the target DNA. Primers for HSV-1 and HSV-2 LAMP were designed against the HSV-1 glycoprotein G (gG) and HSV-2 gG genes, respectively, by using Primer Explorer V software (FUJITSU, Tokyo, Japan), the locations and sequences of which are shown in Table 1. Primer BIP for the gG genes of HSV-1 (HS1BIP) and HSV-2 (HS2BIP) contained the B1 direct sequence and B2 complementary sequence, each specific for the respective strains. Primer FIP for the gG genes of HSV-1 (HS1FIP) and HSV-2 (HS2FIP) contained the F1 complementary sequence and the F2 direct sequence. Primers B3 (HS1B3 and HS2B3) and F3 (HS1F3 and HS2F3) for the HSV-1 and HSV-2 gG genes were located outside the F2-B2 regions. As additional loop primers increase the amplification efficiency (16), loop primers specific for the HSV-1 gG (HS1LPB and HS1LPF) and HSV-2 gG (HS2LPB and HS2LPF) genes were also synthesized. HS1LPB and HS2LPB contained the LPB sequence, while HS1LPF and HS2LPF contained the LPF complementary sequence. The LAMP reaction was performed by using a Loopamp DNA amplification kit (Eiken Chemical, Tochigi, Japan). Reaction mixtures (25 μl) contained 1.6 μM each FIP and BIP primer, 0.8 μM each outer primer (F3 primer and B3 primer), 0.8 μM each loop primer (LPF primer and LPB primer), 2× reaction mix (12.5 μl), *Bst* DNA polymerase (1 μl), and 5 μl of each sample. The mixture was incubated at 63°C for 30 min. Next, a TERAMECS LA200 (Teramecs, Kyoto, Japan) was used to measure turbidity after 30 min of LAMP (15). After turbidity measurement, LAMP products were subjected to electrophoresis on 1.5% agarose gels. Gels were visualized under UV light after ethidium bromide staining. To avoid contamination between samples, different rooms were used for DNA extraction, LAMP setup, and gel analysis using filter-containing pipette tips for aerosol protection. As the turbidities of five negative samples were demonstrated to be 0.01 ± 0.02, we

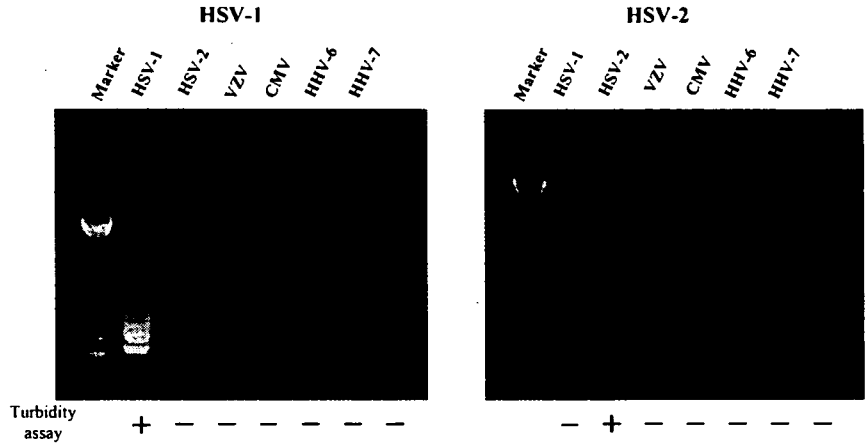

FIG. 1. DNA extracted from HSV-1 (KOS)-, HSV-2 (186)-, VZV (Oka)-, HCMV (AD-169)-, HHV-6 B (Z29)-, and HHV-7 (RK)-infected cells was amplified by using HSV-1- and HSV-2-specific LAMP to determine method specificity. The detection of LAMP products was assessed by agarose gel electrophoresis and turbidity assay using an LA-200. Marker, 123-bp DNA ladder marker.

defined 0.1 as the cutoff value for discrimination between positive and negative samples.

Real-time PCR quantitated the amount of either HSV-1 or HSV-2 DNA in each sample. The genes encoding HSV-1 and HSV-2 glycoprotein G were selected for HSV type-specific real-time PCR. The sequences of the primers and probes used for these experiments were described previously by Pevenstein et al. (20).

To develop an effective assay for rapid measurement of HSV DNA content, we first evaluated the specificity of our HSV type-specific primers. HSV type-specific LAMP was performed on DNA extracted from HSV-1 (KOS)-, HSV-2 (186)-, VZV (Oka)-, HCMV (AD-169)-, HHV-6B (Z29)-, and HHV-7 (RK)-infected cells. As the LAMP products contained several inverted-repeat structures, positive samples exhibit multiple bands of different sizes upon agarose gel electrophoresis. HSV-1-specific primers amplified only HSV-1 DNA and HSV-2-specific primers amplified only HSV-2 DNA (Fig. 1), and no LAMP products were detected in reactions performed with DNA from other viral infections. We also tested the specificity of the primers by using a turbidity assay. The use of HSV-1-specific primers elevated sample turbidity only in HSV-1 DNA-containing samples. Similar specificity was observed for HSV-2-specific primers (Fig. 1).

We also determined the sensitivity of this method. Serial dilutions of either pGEMHS1 or pGEMHS2 plasmid containing the target sequences determined the detection limits of HSV type-specific LAMP. The sensitivities of the HSV-1- and HSV-2-specific LAMP determined by agarose gel electrophoresis were 500 and 1,000 copies/tube, respectively (Fig. 2). Detection by the turbidity assay, however, produced sensitivity levels of 1,000 and 10,000 copies/tube for HSV-1- and HSV-2-specific LAMP, respectively.

After these initial validation studies, we determined the reliability of this HSV type-specific LAMP as a method of viral DNA detection from clinical specimens. Eighteen swab samples (sample numbers 1 to 18) collected from patients with either gingivostomatitis or vesicular skin eruptions were examined (Table 2). Neither HSV-1 nor HSV-2 LAMP products were detected in samples (sample numbers 1 to 8) from which no HSV DNA could be detected by real-time PCR. In contrast, HSV-1 LAMP products were detected by agarose gel electro-

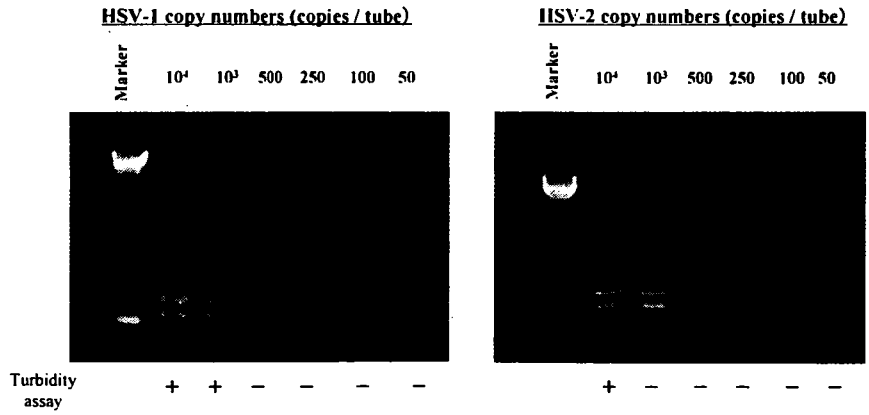

FIG. 2. To determine the respective sensitivities of each assay, serial dilutions of pGEMHS1 and pGEMHS2 plasmid DNAs were amplified by the HSV-1- and HSV-2-specific LAMP, respectively. The detection of LAMP products was assessed by agarose gel electrophoresis and turbidity assay using an LA-200. Marker, 123-bp DNA ladder marker.

TABLE 2. Comparison between HSV type-specific real-time PCR and HSV type-specific LAMP for detection of HSV DNA in swab samples collected from patients with gingivostomatitis or vesicular skin eruptions (samples 1 to 18) and genital HSV infection (samples 19 to 23)

Sample no.	HSV-1[a]					HSV-2[a]				
	Real-time PCR (copies/tube)	LAMP (DNA extraction) result		LAMP (direct[b]) result		Real-time PCR (copies/tube)	LAMP (DNA extraction) result		LAMP (direct[b]) result	
		Agarose gel electrophoresis	Turbidity assay	Agarose gel electrophoresis	Turbidity assay		Agarose gel electrophoresis	Turbidity assay	Agarose gel electrophoresis	Turbidity assay
1	0	−	−	−	−	0	−	−	ND	ND
2	0	−	−	−	−	0	−	−	ND	ND
3	0	−	−	−	−	0	−	−	ND	ND
4	0	−	−	−	−	0	−	−	ND	ND
5	0	−	−	−	−	0	−	−	ND	ND
6	0	−	−	−	−	0	−	−	ND	ND
7	0	−	−	−	−	0	−	−	ND	ND
8	0	−	−	−	−	0	−	−	ND	ND
9	6,350	+	+	+	+	0	−	−	ND	ND
10	9,200	+	−	−	−	0	−	−	ND	ND
11	29,450	+	+	+	+	0	−	−	ND	ND
12	129,650	+	+	+	+	0	−	−	ND	ND
13	194,050	+	+	+	+	0	−	−	ND	ND
14	283,000	+	+	+	+	0	−	−	ND	ND
15	669,950	+	+	+	+	0	−	−	ND	ND
16	2,629,400	+	+	+	+	0	−	−	ND	ND
17	3,769,650	+	+	+	+	0	−	−	ND	ND
18	86,136,700	+	+	+	+	0	−	−	ND	ND
19	0	−	−	ND	ND	641	+	+	−	−
20	0	−	−	ND	ND	22,430	+	+	−	−
21	0	−	−	ND	ND	89,929	+	+	−	−
22	0	−	−	ND	ND	413,117	+	+	−	−
23	0	−	−	ND	ND	443,963	+	+	−	−

[a] +, positive; −, negative.
[b] Swab samples were directly (without DNA extraction) used for LAMP reaction. ND, not done.

phoresis in the 10 HSV-1-positive samples, correlating perfectly with the results of real-time PCR. When the turbidity assay was used, HSV-1 LAMP products were detected in all but 1 (sample number 10) of these 10 positive samples. No HSV-2 DNA could be detected in these samples by either real-time PCR or LAMP. As rapidity and simplicity of the method are critical for commercial and hospital laboratory use, we investigated the requirement for DNA extraction in HSV type-specific LAMP. Either agarose gel electrophoresis or turbidity assay directly detected HSV-1 LAMP product in all 10 swab samples (sample numbers 9 to 18) (sterilized water), with the exception of sample number 10, regardless of the presence or absence of DNA extraction (Table 2). As genital herpes is another important clinical manifestation of herpes infection, we next examined the reliability of HSV type-specific LAMP for the detection of viral DNA in clinical specimens (culture medium) collected from genital lesions (sample numbers 19 to 23) (Table 2). High copy numbers of HSV-2 DNA (ranging between 641 and 443,963 copies/tube) were detected in these samples by HSV-2 type-specific real-time PCR. Both agarose gel electrophoresis and turbidity assay detected HSV-2 LAMP products in all of the samples. To determine the necessity of DNA extraction by this method, we again tried to detect HSV-2 LAMP products in the samples with or without (culture medium) DNA extraction. In contrast, while HSV-2 LAMP products were detected in samples after DNA extraction, no HSV-2 LAMP products were detected in the samples without DNA extraction (Table 2). To determine if the culture medium contained an inhibitor of LAMP, we attempted to detect HSV LAMP products from both sterilized water and culture medium containing plasmid DNA which contained the target sequences. Although both HSV-1 and HSV-2 LAMP products could be detected in sterilized water containing the target sequences, no LAMP products were detected in culture medium containing these DNAs (data not shown).

HSV-1- and HSV-2-specific LAMP specifically amplified HSV-1 and HSV-2 DNA, respectively, exhibiting no cross-reactivity with other human herpesviruses, including another member of the subfamily *Alphaherpesvirinae*, VZV (Fig. 1). This specificity was confirmed by agarose gel electrophoresis and turbidity assay. Although the capability to distinguish between HSV-1 and HSV-2 infection is not crucial for correct administration of antiviral drugs, this discrimination is important from an epidemiological or public health standpoint. As a consequence of the experiment used for determination of the assay sensitivity, it was suggested that the turbidity assay is a less sensitive detection method than agarose gel electrophoresis, as previously suggested (23). However, the turbidity assay is more appropriate for bedside monitoring due to its ease and rapidity. Additionally, turbidity measurement of LAMP products allows a reduction in operation time and reduces contamination risks because of the absence of agarose gel electrophoresis.

We also evaluated the reliability of HSV type-specific LAMP in the detection of viral DNA from different clinical specimens. Although HSV-1 LAMP products were detected by agarose gel electrophoresis in 10 of the 18 swab samples (sterilized water) collected from patients with vesicular skin lesions

and gingivostomatitis suspected as HSV infection, no HSV-2 LAMP products were detected in these samples. All five swab samples (culture medium) collected from the lesions of patients with genital herpes contained HSV-2 LAMP products. These results corresponded well with those from real-time PCR analysis, suggesting that HSV type-specific LAMP is a reliable method for the detection of viral DNA in clinical samples. Although an HSV-1 LAMP product could not be detected in one HSV-1-positive sample by turbidity assay, this inconsistency is probably due to low copy numbers. As the majority of clinical samples (e.g., skin eruptions, oral ulcers, and genital lesions) contain large quantities of viral DNA, the sensitivity of type-specific LAMP by turbidity assay is likely sufficient for the evaluation of most clinical samples. Moreover, all amplification steps are completed within 30 min with an LA-200, and it is a cheaper piece of equipment than that required for real-time PCR, which are major advantages for hospital laboratory use.

Interestingly, when the swabs were collected in sterilized water, HSV LAMP products could be detected directly from the samples without DNA extraction. In contrast, LAMP products could not be detected directly from the culture medium containing viral DNA, regardless of the HSV strain. DNA target sequences, however, became detectable in samples after DNA extraction, suggesting that culture medium contains inhibitors of the LAMP reaction. As the DNA extraction step requires approximately 30 min, omission of DNA extraction could save both time and labor for preparing the samples for LAMP, a major advantage for rapid diagnosis in hospital laboratories. To our knowledge, this is the first report to demonstrate direct amplification of viral DNA from sterilized water containing viral nucleic acids without DNA extraction. We emphasize that the swab should be placed into sterilized water for direct amplification of viral DNA by LAMP. Direct amplification from swab samples in combination with assessment by turbidity assay would accomplish the entire amplification within 30 min. This system would therefore allow large increases in throughput, which is highly relevant for clinical laboratory use. Furthermore, as HSV DNA could be directly detected from swab samples without DNA extraction, the lesions of HSV infection may contain a large quantity of naked viral DNA as well as complete virions. Thus, direct detection of viral DNA from swab samples may be possible by additional DNA amplification methods such as real-time PCR. Further investigation will be necessary to confirm this hypothesis in the future.

We thank Eiken Chemical for their contributions to this work. We also thank Akiko Yoshikawa and Maki Sawamura for their technical assistance.

This work was supported in part by a grant-in-aid for the 21st Century COE Program of Medicine of Fujita Health University and the Open Research Center of Fujita Health University from the Ministry of Education, Culture, Sports, Science, and Technology of Japan and also by a grant-in-aid for scientific research from the Ministry of Education, Science, and Culture of Japan.

REFERENCES

1. **Aldea, C., C. P. Alvarez, L. Folgueira, R. Delgado, and J. R. Otero.** 2002. Rapid detection of herpes simplex virus DNA in genital ulcers by real-time PCR using SYBR green I dye as the detection signal. J. Clin. Microbiol. **40**:1060–1062.
2. **Asano, S., T. Yoshikawa, H. Kimura, Y. Enomoto, M. Ohashi, H. Terasaki, and Y. Nishiyama.** 2004. Monitoring of herpesviruses DNA in three cases of acute retinal necrosis by real-time PCR. J. Clin. Virol. **29**:206–209.
3. **Cone, R. W., A. C. Hobson, J. Palmer, M. Remington, and L. Corey.** 1991. Extended duration of herpes simplex virus DNA in genital lesions detected by the polymerase chain reaction. J. Infect. Dis. **164**:757–760.
4. **Cone, R. W., A. C. Hobson, Z. Brown, R. Ashley, S. Berry, C. Winter, and L. Corey.** 1994. Frequent detection of genital herpes simplex virus DNA by polymerase chain reaction among pregnant women. JAMA **272**:792–796.
5. **Enosawa, M., S. Kageyama, K. Sawai, K. Watanabe, T. Notomi, S. Onoe, Y. Mori, and Y. Yokomizo.** 2003. Use of loop-mediated isothermal amplification of the IS*900* sequence for rapid detection of cultured *Mycobacterium avium* subsp. *paratuberculosis*. J. Clin. Microbiol. **41**:4359–4365.
6. **Espy, M. J., A. D. Wold, D. J. Jespersen, M. F. Jones, and T. F. Smith.** 1991. Comparison of shell vials and conventional tubes seeded with rhabdomyosarcoma and MRC-5 cells for the rapid detection of herpes simplex virus. J. Clin. Microbiol. **29**:2701–2703.
7. **Espy, M. J., J. R. Uhl, P. S. Mitchell, J. N. Thorvilson, K. A. Svien, A. D. Wold, and T. F. Smith.** 2000. Diagnosis of herpes simplex virus infections in the clinical laboratory by LightCycler PCR. J. Clin. Microbiol. **38**:795–799.
8. **Ihira, M., T. Yoshikawa, Y. Enomoto, S. Akimoto, M. Ohashi, S. Suga, Y. Nishimura, T. Ozaki, Y. Nishiyama, T. Notomi, Y. Ohta, and Y. Asano.** 2004. Rapid diagnosis of human herpesvirus 6 infection by a novel DNA amplification method, loop-mediated isothermal amplification. J. Clin. Microbiol. **42**:140–145.
9. **Iwamoto, T., T. Sonobe, and K. Hayashi.** 2003. Loop-mediated isothermal amplification for direct detection of *Mycobacterium tuberculosis* complex, *M. avium*, and *M. intracellulare* in sputum samples. J. Clin. Microbiol. **41**:2616–2622.
10. **Kessler, H. H., G. Muhlbauer, B. Rinner, E. Stelzl, A. Berger, H. W. Dorr, B. Santner, E. Marth, and H. Rabenau.** 2000. Detection of herpes simplex virus DNA by real-time PCR. J. Clin. Microbiol. **38**:2638–2642.
11. **Kimberlin, D. W., F. D. Lakeman, A. M. Arvin, C. G. Prober, L. Corey, D. A. Powell, S. K. Burchett, R. F. Jacobs, S. E. Starr, R. J. Whitley, et al.** 1996. Application of the polymerase chain reaction to the diagnosis and management of neonatal herpes simplex virus disease. J. Infect. Dis. **174**:1162–1167.
12. **Kuboki, N., N. Inoue, T. Sakurai, F. Di Cello, D. J. Grab, H. Suzuki, C. Sugimoto, and I. Igarashi.** 2003. Loop-mediated isothermal amplification for detection of African trypanosomes. J. Clin. Microbiol. **41**:5517–5524.
13. **Lakeman, F. D., R. J. Whitley, et al.** 1995. Diagnosis of herpes simplex encephalitis: application of polymerase chain reaction to cerebrospinal fluid from brain-biopsied patients and correlation with disease. J. Infect. Dis. **171**:857–863.
14. **Mitchell, P. S., M. J. Espy, T. F. Smith, D. R. Toal, P. N. Rys, E. F. Berbari, D. R. Osmon, and D. H. Persing.** 1997. Laboratory diagnosis of central nervous system infections with herpes simplex virus by PCR performed with cerebrospinal fluid specimens. J. Clin. Microbiol. **35**:2873–2877.
15. **Mori, Y., K. Nagamine, N. Tomita, and T. Notomi.** 2002. Detection of loop-mediated isothermal amplification reaction by turbidity derived from magnesium pyrophosphate formation. Biochem. Biophys. Res. Commun. **289**:150–154.
16. **Nagamine, K., T. Hase, and T. Notomi.** 2002. Accelerated reaction by loop-mediated isothermal amplification using loop primers. Mol. Cell. Probes **16**:223–229.
17. **Ndjoyi-Mbiguino, A., F. Ozouaki, J. Legoff, F. X. Mbopi-Keou, A. Si-Mohamed, I. N. Onas, E. Avoune, and L. Belec.** 2003. Comparison of washing and swabbing procedures for collecting genital fluids to assess cervicovaginal shedding of herpes simplex virus type 2 DNA. J. Clin. Microbiol. **41**:2662–2664.
18. **Notomi, T., H. Okayama, H. Masubuchi, T. Yonekawa, K. Watanabe, N. Amino, and T. Hase.** 2000. Loop-mediated isothermal amplification of DNA. Nucleic Acids Res. **28**:e63.
19. **Parida, M., G. Posadas, S. Inoue, F. Hasebe, and K. Morita.** 2004. Real-time reverse transcription loop-mediated isothermal amplification for rapid detection of West Nile virus. J. Clin. Microbiol. **42**:257–263.
20. **Pevenstein, S. R., R. K. Williams, D. McChesney, E. K. Mont, J. E. Smialek, and S. E. Straus.** 1999. Quantitation of latent varicella-zoster virus and herpes simplex virus genomes in human trigeminal ganglia. J. Virol. **73**: 10514–10518.
21. **Ryncarz, A. J., J. Goddard, A. Wald, M. L. Huang, B. Roizman, and L. Corey.** 1999. Development of a high-throughput quantitative assay for detecting herpes simplex virus DNA in clinical samples. J. Clin. Microbiol. **37**:1941–1947.
22. **van Doornum, G. J., J. Guldemeester, A. D. Osterhaus, and H. G. Niesters.** 2003. Diagnosing herpesvirus infections by real-time amplification and rapid culture. J. Clin. Microbiol. **41**:576–580.
23. **Yoshikawa, T., M. Ihira, S. Akimoto, C. Usui, F. Miyake, S. Suga, Y. Enomoto, R. Suzuki, Y. Nishiyama, and Y. Asano.** 2004. Detection of human herpesvirus 7 DNA by loop-mediated isothermal amplification. J. Clin. Microbiol. **42**:1348–1352.

ELSEVIER

Journal of Neuroimmunology 162 (2005) 130–136

Journal of
Neuroimmunology

www.elsevier.com/locate/jneuroim

Autoantibodies against the amino terminal of α-enolase are a useful diagnostic marker of Hashimoto's encephalopathy

A. Fujii[a], M. Yoneda[a,*], T. Ito[b], O. Yamamura[a], S. Satomi[a], H. Higa[c], A. Kimura[d], M. Suzuki[e], M. Yamashita[f], T. Yuasa[d], H. Suzuki[g], M. Kuriyama[a]

[a]*Second Department of Internal Medicine, Faculty of Medical Sciences, University of Fukui, Fukui 910-1193, Japan*
[b]*Department of Cortical Function Disorder, National Institute of Neuroscience, National Center of Neurology and Psychiatry, Tokyo, Japan*
[c]*Department of Internal Medicine, Naha City Hospital, Okinawa, Japan*
[d]*Department of Neurology, Konodai Hospital, National Center of Neurology and Psychiatry, Chiba, Japan*
[e]*Nagasaki-Kamigoshima Hospital, Nagasaki, Japan*
[f]*Department of Neurology, Osaka Saiseikai Nakatsu Hospital, Osaka, Japan*
[g]*Department of Bioscience, Fukui Prefectural University, Fukui, Japan*

Received 19 July 2004; received in revised form 7 February 2005; accepted 7 February 2005

Abstract

We investigated autoantibodies and their epitope(s) in Hashimoto's encephalopathy associated with Hashimoto's thyroiditis. In a proteomic analysis, they proved to recognize α-enolase. We further searched the epitope region in α-enolase using different regions of recombinant proteins expressed in cultured human cells. The amino terminal region was recognized by autobodies from a much higher proportion of patients with Hashimoto's encephalopathy (83.3%; 5/6) than from patients with Hashimoto's thyroiditis (11.8%; 2/17), and not at all by sera from controls (25 healthy individuals and 25 controls with other neurological disorders) (0%; 0/50). Neither the carboxyl terminal nor the mid-region of α-enolase showed specificity for Hashimoto's encephalopathy. Autoantibodies against the amino terminal of α-enolase are a useful diagnostic marker for Hashimoto's encephalopathy.

Keywords: Hashimoto's encephalopathy; Autoantibody; Epitope; α-Enolase; Amino terminal

1. Introduction

A neurological disorder associated with Hashimoto's thyroiditis (HT) has recently come to be regarded as a clinical entity, and named Hashimoto's encephalopathy (HE). HE was originally described by Brain et al., who speculated that an unknown autoimmune mechanism underlies its pathogenesis (Brain et al., 1966). Having carefully observed the relationship between the clinical signs, the change in titers of anti-thyroid antibodies and the endocrine dysfunction in a patient over a long period, Brain and colleagues proposed a new disease entity, HE, which is related to the anti-thyroid antibodies and is clearly distinct from myxoedema encephalopathy associated with hypothyroidism (Brain et al., 1966). Accumulated case reports support this distinction (Shaw et al., 1991; Kothbauer-Margreiter et al., 1996; Peschen-Rosin et al., 1999; Chong et al., 2003; Ferracci et al., 2004).

HE is usually diagnosed based on a combination of neurological findings, the presence of anti-thyroid antibodies, and/or steroid-responsiveness. However, it has a wide spectrum of clinical features including hypertonia, tremors, myoclonus, choreoathetosis, ataxia, seizures, dementia, psychiatric symptoms and stroke. Thus, HE can be underdiagnosed or misdiagnosed as myxoedema encephalopathy, encephalitis, encephalopathy with collagen diseases, paraneoplastic neurological syndromes, cerebrovascular disease, schizophrenia, or even Creutzfeldt–Jakob disease (CJD) (Ghika-Schmid et al., 1996; Wilhelm-Gos-

* Corresponding author. Tel.: +81 776 61 8351; fax: +81 776 61 8110.
E-mail address: myoneda@fmsrsa.fukui-med.ac.jp (M. Yoneda).

0165-5728/$ - see front matter © 2005 Elsevier B.V. All rights reserved.
doi:10.1016/j.jneuroim.2005.02.004

sling et al., 1998; Cossu et al., 2003). Abnormalities of brain MRI/CT and EEG are frequent but heterogeneous in HE, and lack the specificity needed for diagnosing the disease (Shaw et al., 1991; Henchey et al., 1995; Ghika-Schmid et al., 1996; Peschen-Rosin et al., 1999), so more specific diagnostic markers are needed.

An anti-neural antibody against an unknown 34 kDa protein was reported in serum from a HE patient (Oide et al., 2004). Anti-thyroid antibodies and immune complexes were reported in the CSF of HE patients (Ferracci et al., 2003). Thus, antibody-mediated autoimmunity has been speculated to be important in the pathogenesis of HE. Ochi et al. recently identified α-enolase as a candidate target for HE autoantibodies in a proteomic analysis (Ochi et al., 2002). Their report demonstrated that autoantibodies against the full-length recombinant α-enolase expressed in *E. coli* are highly specific in HE. Our own proteomic analysis has also identified α-enolase as a candidate target. We now report that HE autoantibodies specifically recognize its amino terminal and are a useful marker for the diagnosis of HE.

2. Patients and methods

2.1. Patients

The clinical findings of six HE patients are summarized in Table 1. All patients presented with a deterioration in cognition/consciousness, epilepsy, ataxia, tremors, myoclonus or strokes, had serum anti-thyroid antibodies, and responded to steroid therapy. Serum samples from HE patients were studied, and compared with sera from 17 HT patients without any neurological symptoms, 25 healthy individuals and 25 controls with other neurological disorders (5 with encephalitis, 7 with collagen diseases with neurological symptoms, 2 with paraneoplastic neurological syndromes, 4 with multiple sclerosis, 2 with myasthenia gravis, 1 with Wernicke's encephalopathy, 3 with cerebrovascular disease and 1 with CJD). The ethics committee of the University of Fukui approved this research.

2.2. Preparation of proteins for immunological analyses

Human tissues including cerebral white matter, cerebral cortex, cerebellum, liver and thyroid gland were obtained from a 70-year-old woman who died of cerebral embolism in the left middle cerebral artery and underwent an autopsy 3 h postmortem. The unaffected cerebral hemisphere and cerebellum were used for this analysis. Brain tissue was homogenized in 10 mM Tris–HCl, 1 mM ethylene glycol tetraacetic acid (EGTA), with 1 μM phenylmethylsulfonyl fluoride (PMSF), a protease inhibitor.

2.3. SDS–PAGE and immunoblotting

Immunoblotting analysis of the patient's serum against different human tissue lysates including those of cerebral white matter, cerebral cortex, cerebellum, liver and thyroid gland was carried out with 12% sodium lauryl sulfate (SDS)–polyacrylamide gel electrophoresis (PAGE) using a gel electrophoresis system (BE-220, BIO CRAFT, Tokyo, Japan). The proteins on the gel were Western-blotted onto polyvinylidene difluoride (PVDF) membrane (Hybond-P, Amersham Biosciences, NJ) with a blotting apparatus (KS-8453, Oriental Instrument, Tokyo, Japan) at 0.3 mA/cm^2 for 8 h at 4 °C. For detection of the band specific to HE patients, serum was applied to the membrane and incubated in 1% gelatin for 1 h at room temperature, then horseradish peroxidase (HRP)-conjugated anti-human goat IgG Fc (ICN Pharmateuticals, OH) was applied to the membrane as the secondary antibody, fluoresced, and developed on X-ray films (BioMax, Kodak, NY). The serum from a normal individual was used as a control.

2.4. Two-dimensional electrophoresis (2-DE) and immunoblotting

Two-dimensional electrophoresis (2-DE) was carried out using lysate of autopsied human cerebellum in a horizontal electrophoresis system (Multiphor II Electrophoresis Unit, Amersham Biosciences, CA) for the first-dimension isoelectric focusing using an Immobiline DryStrip 7 cm long for the gel, and a linear gradient of p*I* 3–10 (Amersham Biosciences, CA), and was followed by a gel electrophoresis (BE-220, BIO CRAFT, Tokyo, Japan) for the second-dimension SDS–PAGE (12% gel). After the first dimension, the Immobiline gel was incubated in an equilibration buffer (0.05 M Tris–HCl, 6 M urea, 30% glycerol, 1% SDS, 16 mM DTT, and 240 mM iodoacetamide), and subjected to the second-dimension SDS–PAGE (9.5 × 8.5 × 0.1 cm). Immu-

Table 1
The clinical findings of six patients with HE

Number	Patients	Clinical signs	Anti-thyroid Ab	Thyroid function	Protein in CSF	Steroid response
1	57 years, female	disorientation, ataxia, chorea	TPO	euthyroid	normal	excellent
2	44 years, female	disorientation, chorea	TPO	euthyroid	increased	excellent
3	71 years, female	disorientation, seizures	TPO, Tg	euthyroid	increased	excellent
4	71 years, female	coma, strokes	Tg	euthyroid	not examined	fair
5	69 years, female	somnolence, seizures	TPO	euthyroid	increased	good
6	63 years, female	coma, ataxia, myoclonus	Tg	euthyroid	normal	excellent

Ab, antibodies; TPO, anti-thyroid peroxidase Ab; Tg, anti-thyroglobulin Ab.

noblotting was carried out using sera from the HE patients, HT patients and controls as the primary antibody.

2.5. MALDI-TOF/mass spectroscopic analysis

Brain proteins separated by 2-DE were stained with a dye (Zinc Stain kit, BIO-RAD, CA), and the protein spots recognized by serum from an HE patient were removed from the gel, and denatured. The gels were digested with a protease (trypsin), then subjected to a matrix-assisted laser desorption ionization time-of-flight (MALDI-TOF)/mass spectroscopic analysis (Autoflex, Bruker Daltonics, Bremen, Germany or Voyger-DEPR, ABI, CA) for peptide mass fingerprinting (PMF). Protein identification was carried out using a Mascot search (Matrix science, MA) by sending as a query of the PMF data.

2.6. Preparation of recombinant α-enolase proteins in E. coli or cultured human cells

The full-length α-enolase c-DNA was amplified from a human brain cDNA library (Human Brain, whole Marathon-Ready cDNA, CLONTECH, CA) by PCR using a pair of primers encompassing the selected region. The amplified α-enolase cDNA was subcloned into a pGEX plasmid vector (Amasherm Biosciences, CA), Glutathione *S*-transferase (GST)-fusion protein for expression in *E. coli*, or a pcDNA3.1 plasmid vector (Invitrogen, CA) for expression in cultured human cells. The nucleotide sequences of the inserts and cloning junctions were confirmed with a Dye Primer Cycle Sequencing Ready Reaction Kit (Perkin-Elmer, CT). For the preparation of the α-enolase recombinant proteins in an *E. coli* strain (DH5α), 1 μg of the plasmid was transformed by a heat-shock method. The recombinant α-enolase protein was purified using a glutathione sepharose column with a GST Purification kit (Amersham Biosciences, CA), and digested with thrombin to cleave the recombinant protein from the GST.

To locate the epitope of the autoantibody in HE, we expressed regions of α-enolase in HEK cells which may also permit post-translational modifications that would not occur in *E. coli*. The amino (NH_2)-terminal (1–157 amino acids [a.a.]), carboxyl (COOH)-terminal (246–436 a.a.), or mid-region (148–304 a.a.) of α-enolase cDNAs was subcloned into pcDNA3.1 (Invitrogen, CA), a 6xHis-fusion protein expression plasmid vector. Then, 10 μg of the plasmid was precipitated with calcium phosphate and transfected into 5×10^6 cells of HEK293, a human embryonic kidney cell line, in a 10-cm culture dish with Lipofectamine (Invitrogen, CA). Purification of the recombinant α-enolase protein was done through a His column (ProBond Protein Purification kit, Invitrogen, CA).

2.7. Comparison of immunoreactivity with different regions of α-enolase among HE patients, HT patients and controls

Appropriate amounts of different regions of α-enolase expressed in human cells were subjected to SDS–PAGE and immunoblotting. 2-DE was employed for the mid-region

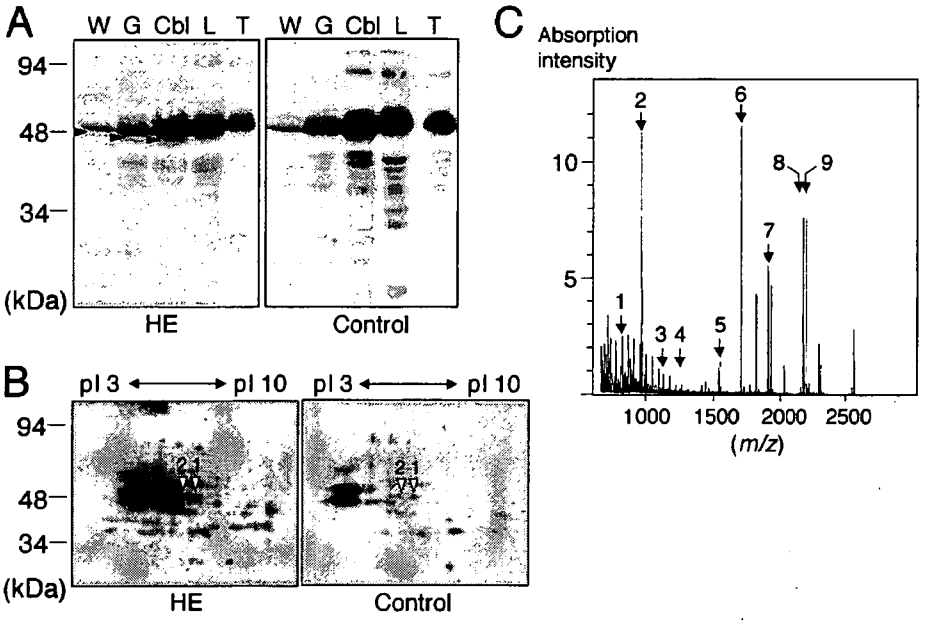

Fig. 1. (A) SDS–PAGE and immunoblotting for the presence of anti-neural antibody in HE. W, brain white matter. G, brain grey matter. Cbl, cerebellum. L, liver. T, thyroid gland. Arrowheads indicate the bands immunoreactive with serum from HE patient 1 in Table 1. (B) Detection of spots immunoreactive with serum from the HE patient on 2-DE. Open arrowheads indicate spot-1 and -2 which have a stronger intensity in HE than in control. (C) MALDI-TOF/mass spectroscopic pattern of the immunoreactive spot-1 digested by trypsin. Nine common signals of mono-isotopic peptides (numbers 1–9 in Table 2), which were obtained by removal of the background noise and repetitive analyses, are indicated by arrows.

Table 2
Mass-fit analysis for typical fragments of the immunoreactive spot in HE

Signal numbers	*m/z* observed	*m/z* expected	Start–end amino acid numbers	Peptide sequences
1	806.41	805.40	309–314	YNQLLR
2	959.53	958.52	329–336	NFRNPLAK
3	1118.69	1117.68	306–314	LAKYNQLLR
4	1259.73	1258.72	23–34	AGAVEKGVPLYR
5	1540.80	1539.79	142–155	VVIGMDVAASEFFR
6	1691.91	1690.90	309–322	YNQLLRIEEELGSK
7	1907.98	1906.98	65–81	LAMQEFMILPVGAANFR
8	2176.08	2175.07	136–155	AGYTDKVVIGMDVAASEFFR
9	2189.16	2188.15	209–229	FTASAGIQVVGDDLTVTNPKR

Selected mass signals for tryptic peptides of spot-1 detected by MALDI-TOF/mass-spectroscopic analysis completely matched the database sequence of tryptic fragments of human α-enolase. The peptide sequences shown in the table were obtained from database sequences of α-enolase, the peptide masses of which matched the search query of tryptic peptide-finger printing. The sequence-matched tryptic peptides covered with 28% of α-enolase. The mass-fit analysis for spot-2 also gave the same results as that for spot-1.

because the signal occasionally overlapped with proteins derived from the cultured human cells from which it was barely distinguishable.

3. Results

3.1. Screening and identification of the target molecule of an HE patient's autoantibodies

To screen for the target molecule that reacted selectively with serum from HE patient 1 in Table 1, SDS–PAGE and immunoblotting were employed. In Fig. 1A, a 48 kDa protein shows stronger blotting signals with serum from the HE patient than from a control. It appears to be restricted to brain tissues. The cerebellum protein lysate was subjected to 2-DE, and two spots with the same molecular weight and different p*I* values were identified that gave stronger blotting intensities with the HE than the control serum (Fig. 1B). These two spots were further subjected to MALDI-TOF/mass spectroscopic analysis. Fig. 1C and Table 2 show the MALDI-TOF mass spectra of immunoreactive spot-1 and its mass-fit analysis data, respectively. α-Enolase was identified in two spots with a slightly different p*I*, probably due to post-translational modifications. These results demonstrated that α-enolase was a candidate target molecule reactive with serum from the HE patient.

3.2. Immunoreactivity of sera from HE patients, HT patients and controls with full-length recombinant α-enolase expressed in E. coli or cultured human cells

All of the sera from HE patients, HT patients and controls reacted with the "full-length" α-enolase expressed in *E. coli* with varying signal intensities (Fig. 2A). The sera from HE and HT patients also reacted with the full-length α-enolase expressed in cultured human cells, and there was even discordant reactivity with the control sera (Fig. 2B). However, the same serum sometimes reacted with recombinant proteins from *E. coli* and cultured human cells. All recombinant full-length α-enolase expressed in *E. coli* reacted with control sera ($n=15$), whereas some of the expressed one in cultured human cells reacted with control sera (2/8; 25%).

3.3. Comparison of immunoreactivity of various regions of α-enolase among HE patients, HT patients and controls

To locate the serological epitope(s) in the α-enolase, various regions of recombinant proteins were expressed in cultured human cells, purified on a Ni column, and subjected to SDS–PAGE (Fig. 3A). The NH_2-terminal, COOH-terminal and mid-regions of the recombinant α-enolase were clearly identified with an anti-His antibody, which verified their expression (Fig. 3A, left panel). A commercially available monoclonal antibody against α-enolase only reacted with the COOH-terminal region (Fig. 3A, 2nd left panel).

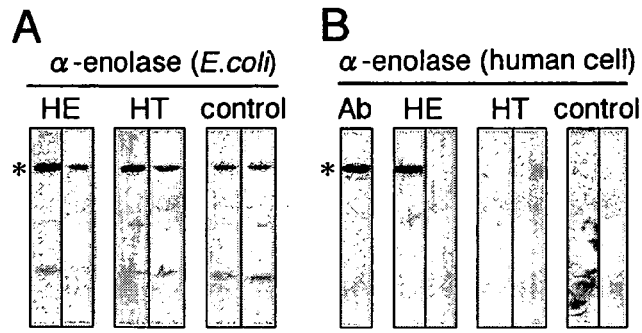

Fig. 2. (A) Immunoblotting of the full-length recombinant α-enolase expressed in *E. coli* with sera from HE patients 1 and 2 (Table 1), HT patients or healthy controls. An asterisk indicates the full-length recombinant α-enolase expressed in *E. coli*. (B) Immunoblotting of the full-length recombinant α-enolase expressed in cultured human cells with sera from HE patients 1 and 2, two HT patients or two controls. Ab, a commercially available monoclonal anti-α-enolase antibody (sc-7455, Santa Cruz Biotechnology, CA). An asterisk indicates the full-length recombinant α-enolase expressed in human cultured cells.

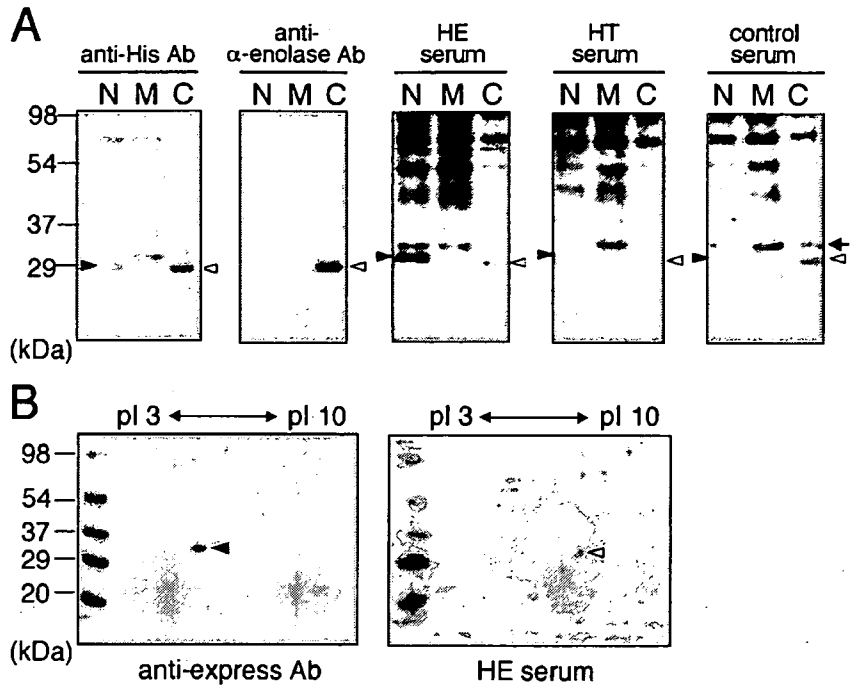

Fig. 3. (A) Immunoblotting of various regions of α-enolase with sera from HE and HT patients and a control. Recombinant α-enolase regions were expressed in cultured human cells. N, recombinant NH_2-terminal region of α-enolase. M, recombinant mid-region of α-enolase. C, recombinant COOH-terminal region of α-enolase. Anti-His Ab, immunoblotting with an anti-Histidine antibody. Anti-α-enolase Ab, immunoblotting with a commercially available monoclonal anti-α-enolase antibody (sc-7455, Santa Cruz Biotechnology, CA). HE serum, immunoblotting with serum from HE patient 1 (Table 1). HT serum, immunoblotting with serum from a patient with HT without any neurological signs. Control serum, immunoblotting with serum from a normal control. Arrowheads indicate the NH_2-terminal region. Open arrowheads indicate the COOH-terminal region. An arrow indicates signals derived from cultured human cells. (B) 2-DE of the recombinant mid-region of α-enolase expressed in cultured human cells, and lack of immunoreactivity with serum from a patient with HE. Anti-expression antibody, a commercially available monoclonal antibody recognizing the region between the His tag and cloning site (Anti-Xpress Antibody, Invitrogen, CA). An arrowhead indicates the recombinant mid-region of α-enolase. An open arrowhead indicates the band imunoreactive with serum from an HE patient.

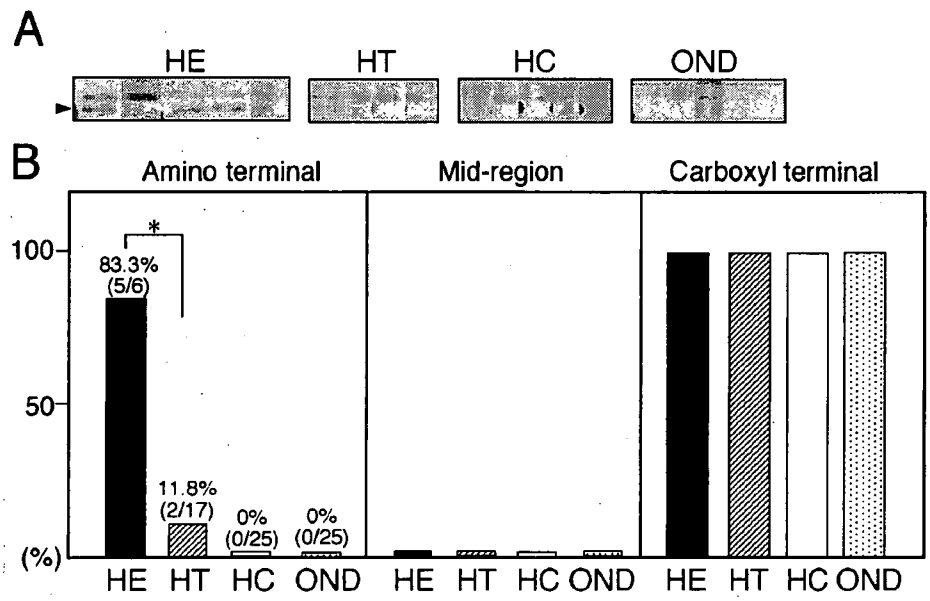

Fig. 4. (A) Immunoblotting of the recombinant NH_2-terminal region of α-enolase expressed in cultured human cells with sera from patients with HE or HT, or from controls. HE, sera from HE patients 1–5 in Table 1. HT, sera from HT patients. HC, sera from healthy controls. OND, sera from controls with other neurological disorders. OND includes patients with encephalitis, encephalopathy with collagen disease, multiple sclerosis, CJD and cerebrovascular disease. Arrowheads indicate the signals reactive with the NH_2-terminal region. (B) Percentages of sera from patients with HE or HT, or from controls, reactive with different regions of recombinant α-enolase expressed in cultured human cells. $*p<0.005$. HE, $n=6$; HT, $n=17$; HC, $n=25$; OND, $n=25$ in amino terminal region, $n=15$ in mid-region and carboxyl terminal region.

The NH_2-terminal of the recombinant α-enolase reacted with sera from HE patients, but rarely from HT patients or controls (Fig. 3A, the panels 3–5). By contrast, the COOH-terminal of the recombinant α-enolase reacted with all sera tested. The mid-region did not react with any human sera, though it gave a strong signal at the expected position with the commercially available monoclonal antibody at one end (Fig. 3B).

3.4. Percentages of serum samples from HE patients, HT patients and controls immunoreactive with various regions of α-enolase

The recombinant NH_2-terminal region of α-enolase was highly reactive in HE patients 1–5 (Table 1) (5 out of 6; 83.3%), much less reactive in HT (2 out of 17; 11.8%), and unreactive in 25 healthy controls and 25 controls with other neurological disorders (p value <0.005 between HE and HT; Fisher's exact test) (Fig. 4). In contrast, the COOH-terminal reacted with all sera, and the mid-region did not react with any of them (Fig. 4). These results demonstrate that the NH_2-terminal region of α-enolase contains an immunoreactive site.

4. Discussion

Searching for specific autoantibodies in sera from HE patients, we identified an antibody against a 48 kDa molecule in an HE patient on SDS–PAGE and 2-DE (Fig. 1A and B). The patient's serum reacted with the 48 kDa protein in brain tissues, suggesting the existence of an anti-neuronal antibody (Fig. 1A). Two-DE revealed two spots with the same molecular weight and slightly different p*I* values, which showed stronger reactivity with HE than the control sera (Fig. 1B). MALDI-TOF/mass spectroscopic analysis identified α-enolase sequences in these two spots (Fig. 1C; Table 2). This suggests that α-enolase is a candidate target for HE autoantibodies, which may recognize post-translationally modified forms. Recently, Ochi et al. also identified α-enolase as a possible target for antibodies in sera from patients with HE, in a proteomic analysis (Ochi et al., 2002).

To locate epitope(s) in α-enolase that react with the autoantibodies in HE patients, we tested the NH_2-terminal, COOH-terminal and mid-regions. These regions were expressed in cultured human cells because a nascent polypeptide undergoes natural post-translational modifications possibly influencing the conformation of the protein concerned with the autoimmunity, as compared with the absence in *E. coli*. Remarkably, the recombinant NH_2-terminal of α-enolase was recognized by sera from 5/6 HE patients (83.3%) but only 2/17 HT patients (11.8%) and 0% of healthy individuals and controls with other neurological disorders (p<0.005 between HE and HT) (Fig. 4). These results clearly demonstrate that the autoantibodies in HE patients specifically recognize a key epitope in the NH_2-terminal region of α-enolase.

In sharp contrast, the sera from all patients and controls apparently reacted non-specifically with the recombinant COOH-terminal region and full-length α-enolase, but did not react detectably with its mid-region (Fig. 4).

Notably, however, when Ochi et al. used full-length α-enolase expressed in *E. coli*, they detected autoantibodies more often in sera from HE patients (60%) than from HT patients (6%) or controls (0%) (Ochi et al., 2002). This apparently specific recognition contrasts starkly with the non-specific binding that we found between control sera and full-length recombinant α-enolase, even after expression in human cells, which argues against influences from *E. coli* components. The reasons are not clear, but the 'stickiness' appears to be localized to the region form 246 to 436. Possibly (a) this region somehow masks the specific epitope within 1–157 when full-length recombinant products are tested or (b) this masking was avoided by Ochi et al. because of differences in re-folding or in proteolysis. If post-translational modifications are involved, they must differ between human brain and *E. coli*. They might include the conversion of amide side-chains (i.e. Gln or Asn to Glu or Asp) in the protein, which is sometimes necessary for T cell recognition (Anderson et al., 2000), or glycosylation of the protein. The number of Gln is 1 in the amino terminal region, 2 in the mid-region and 9 in the carboxyl terminal region of α-enolase; while the number of Asn is 4 in the amino terminal region, 9 in the mid-region and 5 in the carboxyl terminal region.

The enolases are cytosolic enzymes and play an important role in the glycolytic pathway in all cells (Lebioda and Stec, 1991). The functional enzyme is a dimer made up of subunits referred to as α, β and γ. In mammals there are at least three isoforms of enolase characterized by different tissue distributions as well as by distinct biochemical and immunologic properties. The α-enolase is a nearly ubiquitous form, found in almost all tissues, and its expression precedes that of the other isoforms in the early stage of embryonic development. The β-enolase is present in adult skeletal muscle, and the γ-enolase is the major form found in mature neurons and in cells of neuronal origin (Lebioda and Stec, 1991). However, it is thought to be a multifunctional protein and also has potential roles in autoimmune disorders (Pancholi, 2001; Moscato et al., 2000; O'Dwyer et al., 2002). α-Enolase apparently serves as a plasminogen receptor on the surface of a variety of hematopoetic, epithelial and endothelial cells, suggesting that it plays an important role in the intravascular and pericellular fibrinolytic systems (Pancholi and Fischetti, 1998). Indeed, vasculitis was reported in an autopsy case of HE (Nolte et al., 2000). In addition, this protein can act as a heat-shock protein and bind cytoskeletal and chromatin structures, implying crucial roles in transcription and a variety of pathophysiological processes (Subramanian and Miller, 2000).

The NH_2-terminal region of α-enolase is located on the extruding part of the enzyme and is important for intermolecular interactions (Lebioda and Stec, 1991), and evidently includes a major serological epitope. Although it is unclear whether α-enolase, a cytosolic protein, is expressed on the cell surface or not, it could be released from the cytosol to the outside of cells by destruction of the thyroid gland (i.e. thyroiditis), and so come into contact with immune cells.

In conclusion, the NH_2-terminal region of α-enolase is a novel target for autoantibodies in HE, and may be subject to post-translational modifications. These autoantibodies appear to be a useful diagnostic marker of HE.

Acknowledgements

We would like to thank Prof. Takashi Inuzuka, Gifu University, Dr. Keiko Tanaka, Niigata University and Dr. Kiyotoshi Kaneko, National Center of Neurology and Psychiatry for technical advice, and to Tomomi Kame for technical assistance. This work was supported in part by a grant from the Ministry of Health, Labor and Welfare of Japan (to MY).

References

Anderson, R.P., Degano, P., Godkin, A.J., Jewell, D.P., Hill, A.V.S., 2000. In vivo antigen challenge in celiac disease identifies a single transglutaminase-modified peptide as the dominant A-gliadin T-cell epitope. Nat. Med. 6, 337–342.

Brain, L., Jellinek, E.H., Ball, K., 1966. Hashimoto's disease and encephalopathy. Lancet ii, 512–514.

Chong, J.Y., Roland, L.P., Utiger, R.D., 2003. Hashimoto encephalopathy. syndrome or myth? Arch. Neurol. 60, 164–171.

Cossu, G., Melis, M., Molari, A., Pinna, L., Ferringo, P., Melis, G., Zonza, F., Spissu, A., 2003. Creitzfeldt–Jakob disease associated with high titter of antithyroid autoantibodies: case report and literature review. Neurol. Sci. 24, 138–140.

Ferracci, F., Moretto, G., Candeago, R.M., Cimini, N., Conte, F., Gentile, M., Papa, N., Carnevale, A., 2003. Antithyroid antibodies in the CSF: their role in the pathogenesis of Hashimoto's encephalopathy. Neurology 60, 712–714.

Ferracci, F., Bertiato, G., Moretto, G., 2004. Hashimoto's encephalopathy: epidemiologic data and pathogenetic considerations. J. Neurol. Sci. 217, 165–168.

Ghika-Schmid, F., Ghika, J., Regli, F., Dworak, N., Bogousslavsky, J., Stadler, C., Portmann, L., Despland, P.A., 1996. Hashimoto's myoclonic encephalopathy: an underdiagnosed treatable condition? Mov. Disord. 11, 555–562.

Henchey, R., Cibula, J., Helveston, W., Malone, J., Gilmore, R.L., 1995. Electroencephalographic findings in Hashimoto's encephalopathy. Neurology 45, 977–981.

Kothbauer-Margreiter, I., Sturzenegger, M., Komor, J., Baumgartner, R., Hess, C.W., 1996. Encephalopathy associated with Hashimoto thyroiditis: diagnosis and treatment. J. Neurol. 243, 585–593.

Lebioda, L., Stec, B., 1991. Mapping of isozymic differences in enolase. Int. J. Biol. Macromol. 13, 97–100.

Moscato, S., Pratesi, F., Sabbatini, A., Chimenti, D., Scavuzzo, M., Passatino, R., Bombardieri, S., Giallongo, A., Migliorini, P., 2000. Surface expression of a glycolytic enzyme, alpha-enolase, recognized by autoantibodies in connective tissue disorders. Eur. J. Immunol. 30, 3575–3584.

Nolte, K.W., Unbehaun, A., Sieker, H., Kloss, T.M., Paulus, W., 2000. Hashimoto encephalopathy: a brainstem vasculitis? Neurology 54, 769–770.

Ochi, H., Horiuchi, I., Araki, N., Toda, T., Araki, T., Sato, K., Murai, H., Osoegawa, M., Yamada, T., Okamura, K., Ogino, T., Mizumoto, K., Yamashita, H., Saya, H., Kira, J., 2002. Proteomic analysis of human brain identifies alpha-enolase as a novel autoantigen in Hashimoto's encephalopathy. FEBS Lett. 528, 197–202.

O'Dwyer, D.T., Smith, A.I., Matthew, M.L., Andronicos, N.M., Ranson, M., Robinson, P.J., Crock, P.A., 2002. Identification of the 49-kDa autoantigen associated with lymphocytic hypophysitis as alpha-enolase. J. Clin. Endocrinol. Metab. 87, 752–757.

Oide, T., Tokuda, T., Yazaki, M., Watarai, M., Mitsuhashi, S., Kaneko, K., Hashimoto, T., Ohara, S., Ikeda, S., 2004. Anti-neuronal autoantibody in Hashimoto's encephalopathy: neuropathological, immunohistochemical, and biochemical analysis of two patients. J. Neurol. Sci. 217, 7–12.

Pancholi, V., 2001. Multifunctional alpha-enolase: its role in diseases. Cell. Mol. Life Sci. 58, 902–920.

Pancholi, V., Fischetti, V.A., 1998. Alpha-enolase, a novel strong plasmin(ogen) binding protein on the surface of pathogenic streptococci. J. Biol. Chem. 273, 14503–14515.

Peschen-Rosin, R., Schabet, M., Dichgans, J., 1999. Manifestation of Hashimoto's encephalopathy years before onset of thyroid disease. Eur. Neurol. 41, 79–84.

Shaw, P.J., Walls, T.J., Newman, P.K., Cleland, P.G., Cartlidge, N.E.F., 1991. Hashimoto's encephalopathy: a steroid-responsive disorder associated with anti-thyroid antibody titers—report of 5 cases. Neurology 41, 228–233.

Subramanian, A., Miller, D.M., 2000. Structural analysis of alpha-enolase. Mapping the functional domains involved in down-regulation of the c-myc protooncogene. J. Biol. Chem. 275, 5958–5965.

Wilhelm-Gossling, C., Weckbecker, K., Brabant, E.G., Denglerm, R., 1998. Autoimmune encephalopathy in Hashimoto's thyroiditis. A differential diagnosis in progressive dementia syndrome. Dtsch. Med. Wochenschr. 123, 279–284.

ELSEVIER

Journal of the Neurological Sciences 239 (2005) 53 – 57

Journal of the Neurological Sciences

www.elsevier.com/locate/jns

Analysis of serum soluble CD40 ligand in patients with influenza virus-associated encephalopathy

Takashi Ichiyama [a,*], Tsuneo Morishima [b], Naoko Suenaga [a], Madoka Kajimoto [a], Tomoyo Matsubara [a], Susumu Furukawa [a]

[a] *Department of Pediatrics, Yamaguchi University School of Medicine, 1-1-1 Minamikogushi, Ube, Yamaguchi 755-8505, Japan*
[b] *Department of Pediatrics, Okayama University Graduate School of Medicine and Dentistry, Japan*

Received 17 May 2005; received in revised form 20 July 2005; accepted 25 July 2005
Available online 6 September 2005

Abstract

CD40 ligand (CD40L) is mainly expressed on activated platelets and CD4+T cells, and it can be cleaved from the cell surface, releasing a soluble CD40L (sCD40L). Most sCD40L is derived from activated platelets. A previous paper revealed that the platelet number of patients with influenza virus-associated encephalopathy (IE) was correlated with the outcome. We determined the utility of sCD40L as a predictor for the prognosis of IE. We measured the serum concentration of sCD40L and the platelet number on the day of hospitalization in 34 patients with IE, 16 with influenza virus-associated febrile seizures (IFS), 19 with influenza virus infection without complications (Flu), and 7 with Epstein–Barr virus (EBV) infection. The serum sCD40L concentrations in IE and IFS were significantly lower than those in controls, Flu, and EBV infections. Serum sCD40L concentrations in the IE group were 0.70±0.43 ng/ml for deceased patients, 1.73±1.36 ng/ml for those with sequelae, and 3.85±2.91 ng/ml for those without sequelae. There was no significant difference in platelet number between IE patients with and without sequelae, while the platelet number of deceased patients with IE was significantly lower than in controls, Flu, and IFS. Serum sCD40L concentration on the day of hospitalization was more correlated with the outcome of IE than platelet number. Our findings suggest that the serum sCD40L concentration during acute IE is important for predicting the prognosis at an early stage.

Keywords: Epstein–Barr virus; Influenza virus-associated encephalopathy; Platelet; Soluble CD40 ligand

1. Introduction

CD40 ligand (CD40L) is a transmembrane protein expressed on activated platelets and CD4+T cells [1,2]. CD40L can be cleaved from the cell surface, releasing a soluble CD40L (sCD40L) which is biologically active [2,3]. Several previous papers demonstrated that most serum sCD40L is derived from platelets [4–6].

Many patients with influenza virus-associated encephalopathy (IE) have been reported in Japan [7–9], and recently, some cases have been reported in Europe and the United States [10,11]. Pathological findings revealed that viral antigens and inflammatory cells were undetectable in brain tissues and suggest that direct viral invasion does not induce IE [12,13]. Serum and CSF concentrations of several proinflammatory cytokines and cytokine receptors, such as interleukin-6 (IL-6), IL-1β, and soluble tumor necrosis factor (TNF) receptor 1, are elevated and related to the clinical severity of IE [14–16]. Moreover, the platelet number tends to be correlated with the outcome of IE [8,12,17]. To evaluate the utility of sCD40L in the severity and prognosis of IE, we measured the serum sCD40L concentrations on the day of hospitalization in patients with IE, influenza virus-associated febrile seizures (IFS), influenza virus infection without complications (Flu), and Epstein–Barr virus (EBV) infection.

* Corresponding author. Tel.: +81 836 22 2258; fax: +81 836 22 2257.
E-mail address: ichiyama@yamaguchi-u.ac.jp (T. Ichiyama).

0022-510X/$ - see front matter © 2005 Elsevier B.V. All rights reserved.
doi:10.1016/j.jns.2005.07.010